Entanglement entropy in quantum impurity systems and systems with boundaries

2009 J. Phys. A: Math. Theor. 42 504009

(http://iopscience.iop.org/1751-8121/42/50/504009)

IOP PUBLISHING JOURNAL OF PHYSICS A: MATHEMATICAL AND THEORETICAL

J. Phys. A: Math. Theor. **42** (2009) 504009 (36pp) doi:10.1088/1751-8113/42/50/504009

Entanglement entropy in quantum impurity systems and systems with boundaries

Ian Affleck[1], **Nicolas Laflorencie**[2] **and Erik S Sørensen**[3]

[1] Department of Physics and Astronomy, University of British Columbia, Vancouver, BC, V6T 1Z1, Canada
[2] Laboratoire de Physique des Solides, Université Paris-Sud, UMR-8502 CNRS, 91405 Orsay, France
[3] Department of Physics and Astronomy, McMaster University, Hamilton, ON, L8S 4M1, Canada

E-mail: iaffleck@physics.ubc.ca, laflorencie@lps.u-psud.fr and sorensen@mcmaster.ca

Received 9 June 2009, in final form 16 October 2009
Published 2 December 2009
Online at stacks.iop.org/JPhysA/42/504009

Abstract

We review research on a number of situations where a quantum impurity or a physical boundary has an interesting effect on entanglement entropy. Our focus is mainly on impurity entanglement as it occurs in one-dimensional systems with a single impurity or a boundary, in particular quantum spin models, but generalizations to higher dimensions are also reviewed. Recent advances in the understanding of impurity entanglement as it occurs in the spin-boson and Kondo impurity models are discussed along with the influence of boundaries. Particular attention is paid to $(1+1)$-dimensional models where analytical results can be obtained for the case of conformally invariant boundary conditions and a connection to topological entanglement entropy is made. New results for the entanglement in systems with mixed boundary conditions are presented. Analytical results for the entanglement entropy obtained from Fermi liquid theory are also discussed as well as several different recent definitions of the impurity contribution to the entanglement entropy.

PACS numbers: 03.67.Mn, 75.30.Hx, 75.10.Pq

(Some figures in this article are in colour only in the electronic version)

1. Introduction

The definition of entanglement entropy is based on dividing space into two regions. In many cases, the systems under study are homogeneous and this division is purely fictitious. However, there has also been considerable activity on studying entanglement in inhomogeneous systems, the simplest of which contain physical boundaries or a single impurity. There are currently several useful measures of entanglement; here we shall use the von Neumann entanglement

entropy as defined by dividing a bipartite system in a pure state at $T = 0$ into two regions, A and B. From the ground state pure density matrix, region B is traced over to define the reduced density matrix ρ_A. In most cases, we shall take A to include the impurity/boundary. From this, the von Neumann entanglement entropy [1, 2]

$$S(r, R) \equiv -\mathrm{Tr}[\rho_A \ln \rho_A] \tag{1.1}$$

is obtained for a subsystem of size r inside a larger system of size R. There are several motivations for this work.

One motivation is to study models of a qubit interacting with a decohering environment [3–7]. Such a system is often represented by a two-level system, or spin-1/2, interacting with an otherwise homogeneous, and often one-dimensional medium with gapless excitations. Some versions of this model are equivalent to the Kondo model, motivating studies of ground state entanglement of an impurity spin with the conduction electrons in Kondo models. This entanglement entropy can be easily expressed exactly in terms of the impurity magnetization, which, for many models, has been well understood many years ago [5, 8]. This single site impurity entanglement, which we denote by s_{imp}, is reviewed in section 2.

Another motivation comes from the thermodynamic impurity entropy, $\ln g$, which was calculated by Bethe ansatz [9, 10] for multi-channel Kondo models and then discussed more generally from the viewpoint of conformal field theory (CFT) [11]. General quantum impurity models, as in condensed matter physics, were argued to renormalize to conformally invariant boundary conditions, and $\ln g$ was argued to be a universal quantity depending only on the boundary condition. Calabrese and Cardy (C&C) [12] argued that, for a CFT defined on the semi-infinite line with a conformally invariant boundary condition (CIBC) at the end, the entanglement of a region of length r with the rest is given by [12–15]

$$S(r) = \frac{c}{6} \ln\left(\frac{r}{a}\right) + \ln g + s_1/2. \tag{1.2}$$

$\ln g$ depends on the CIBC, establishing a surprising connection between thermodynamic and entanglement entropy. Here, a is a cut-off length scale and s_1 is a non-universal number. Both are independent of the CIBC. In the numerical work, one-dimensional tight binding models are generally considered in which case a is the lattice constant. This raised the possibility that this impurity part of the entanglement entropy, S_{imp}, might exhibit universal renormalization group (RG) behavior and this was confirmed in studies of spin chains with a boundary magnetic field [16] and of the Kondo model [8, 17]. The connection between the thermodynamic impurity entropy and the impurity entanglement entropy is outlined in section 3.

There is a deep connection between (1+1)-dimensional CFT and topological phases of gapped (2+1)-dimensional systems such as that in the fractional quantum Hall effect. While the entanglement entropy of a region in a gapped two-dimensional (2D) system is expected to grow with the length of its perimeter, it was shown that there is an additional universal, length-independent 'topological entropy' [18, 19], $-\ln \mathcal{D}$ which can be extracted from the corresponding (1+1)-dimensional CFT. The connection between the boundary entropy of C&C [12] and the topological entropy can be clarified by considering a (2+1)-dimensional system with boundaries, a 'Hall bar', containing a point contact. There are gapless degrees of freedom living on the edge of the Hall bar described by a CFT. (See figure 9.) The point contact may renormalize to a CIBC, corresponding to breaking the Hall bar into two pieces and the change in topological entropy due to this renormalization can be related to the change in the boundary entropy, $\ln g$. As we will show, this is defined in terms of the entanglement of a section of the Hall bar of length r, containing the point contact with the rest of the (infinite) Hall bar. The connection with topological phases is discussed in section 3.3.

An alternative type of impurity-related entanglement entropy has also been studied for a 1D wire with a point defect, which, if relevant, effectively breaks the system into two at low

energies [20–22]. Rather than studying the entanglement of a finite region surrounding the point contact and extracting the $\ln g$ term in equation (1.2) instead the entanglement of one side of the point contact with the other was studied. In cases where the point defect is relevant, it was found that this entanglement tends to vanish with increasing system size, again verifying that entanglement entropy exhibits RG flow behavior. This type of impurity entanglement is discussed in section 4.

A surprising result of numerical studies of entanglement entropy in 1D antiferromagnets with boundaries was the presence of an alternating term decaying away from the boundaries [8, 23]. Although a theory of this is still lacking, it was shown numerically to track closely the energy density as a function of distance from the boundary and a heuristic understanding was obtained in terms of a local dimerization induced by the boundary, related to 'resonating valence bonds'. This boundary-induced alternation in the entanglement entropy is reviewed in section 5.

Although probably less useful as a model of a decohering environment and not related to CFT and universal RG concepts, impurity entanglement entropy has also been studied for gapped (1+1)-dimensional systems, including dimerized and Haldane gap spin chains. This aspect is reviewed in section 6.

As a final motivation, we note that recent models for qubit teleportation and quantum state transfer using quantum spin chains [24–34] employ models closely related to the quantum spin models reviewed and in many cases rely on properties of the entanglement arising from the impurities reviewed here.

Recently there has been some very interesting work on time-dependent entanglement entropy following a local quench, which also involves systems with quantum impurities [35–38]. However, this is reviewed in another article in this series [39], so we do not review it here.

2. The single site impurity entanglement entropy, s_{imp}

The simplest definition of the impurity entanglement is to consider the (single site) impurity as sub-system A and the rest of the system as sub-system B. A measure of the impurity entanglement is then simply given by the von Neumann entanglement entropy of the reduced density matrix for A inside a system of total size R. Since A describes just a single site one often refers to this as the single site impurity entanglement. We shall denote this quantity by s_{imp} to distinguish it from $S_{\mathrm{imp}}(r, R)$ defined in later sections by the *difference* in the *uniform* part of the von Neumann entanglement entropy for a sub-system of extent r with and without the impurity present. Since s_{imp} is concerned with a single site, such a definition through a subtraction is not possible and the explicit r dependence through the size of the sub-system A is absent.

The single site impurity entanglement, s_{imp}, has been studied mainly in two different settings: the spin-boson model [4–6, 40] and the closely related Kondo model [8]. For the case where the impurity is a $s = 1/2$ system (qubit), it is easy to see [4, 8, 40] that

$$s_{\mathrm{imp}} = -\sum_{\pm}(1/2 \pm m_{\mathrm{imp}}) \ln[(1/2 \pm m_{\mathrm{imp}})], \tag{2.1}$$

m_{imp} being the magnetization of the impurity in the ground state. In this case s_{imp} only recasts m_{imp}. For completeness we give here an explicit proof. For the case of a singlet ground state, we may write the ground state as $\left(\left|\frac{1}{2}, -\frac{1}{2}\right\rangle - \left|-\frac{1}{2}, \frac{1}{2}\right\rangle\right)/\sqrt{2}$. Here the first $1/2$ is S^z_{imp}. The rest of the system is in a state of spin $S = 1/2$ with $S^z = \pm 1/2$. The second fraction gives the S^z quantum number of the rest of the system. Clearly this gives entanglement entropy $\ln(2)$ and

zero impurity magnetization. For the case of a $S = 1/2$ ground state, the rest of the system can be in a state of spin 0 or 1 only. For the case of $S^z_{\rm Total} = +1/2$, the ground state can be written as $a|\frac{1}{2}; 0, 0\rangle + b\big(|\frac{1}{2}; 1, 0\rangle - |-\frac{1}{2}; 1, 1\rangle\big)$. Here the second number is the S quantum number of the rest of the system and the third is the S^z quantum number. The relative coefficient of the second and third terms is fixed by the requirement of having a state of total spin $S_{\rm Total} = 1/2$. $|a|^2 + 2|b|^2 = 1$ for the state to be normalized. The reduced density matrix is diagonal with entries $|a|^2 + |b|^2$ and $|b|^2$. Thus, the entanglement entropy is $-\ln(|a|^2 + |b|^2) - \ln|b|^2$ and $m_{\rm imp} = (1/2)|a|^2$. The result equation (2.1) follows.

For a system with a singlet ground state $m_{\rm imp} = 0$ and $s_{\rm imp}$ is maximal [3], the qubit is maximally entangled with the rest of the system. For a system with a doublet ground state (R odd) the behavior of $m_{\rm imp}$ is more interesting and exhibits the usual crossover associated with Kondo physics. In this case, $m_{\rm imp}$ was studied, for the usual fermion Kondo model, in [41] and [42, 43] for example from which $s_{\rm imp}$ can be derived.

The spin-boson model with a level asymmetry h is defined by

$$H_{\rm SB} = -\frac{\Delta}{2}\sigma_x + \frac{h}{2}\sigma_z + H_{\rm osc} + \frac{1}{2}\sigma_z \sum_q \lambda_q (a_q + a_q^\dagger), \tag{2.2}$$

where σ_x and σ_z are Pauli matrices and Δ is the tunneling amplitude between the states with $\sigma_z = \pm 1$. $H_{\rm osc}$ is the Hamiltonian of an infinite number of harmonic oscillators with frequencies $\{\omega_q\}$, which couple to the spin degree via $\{\lambda_q\}$. The heat bath is characterized by its spectral function $J(\omega) \equiv \pi \sum_q \lambda_q^2 \delta(\omega_q - \omega) = 2\pi\alpha\omega,\ \omega \ll \omega_c$ (Ohmic heat bath). Efficient NRG calculations can be performed on this model through a mapping [44] to the anisotropic Kondo model. This allowed for rather detailed NRG studies [40] of $s_{\rm imp}$ as a function of α. Exploiting known exact results for $\langle\sigma_z\rangle$ and $\langle\sigma_x\rangle$ in the spin-boson problem, it has been shown [4] that $s_{\rm imp}$ in several limits is a *universal* function of h/T_K, where T_K is the Kondo scale. For $T_K \ll h \ll \Delta$, it was found [4] that

$$\lim_{T_K \ll h \ll \Delta} s_{\rm imp}(\alpha, \Delta, h) = k_2(\alpha) \left(\frac{T_K}{h}\right)^{2-2\alpha} \ln\left(\frac{h}{T_K}\right), \tag{2.3}$$

with $k_2(\alpha)$ being a known cut-off independent function so that $s_{\rm imp}$ in this limit is a universal function of h/T_K. On the other hand, for $h \ll T_K \ll \Delta$ it can be shown that

$$\lim_{h \ll T_K \ll \Delta} s_{\rm imp}(\alpha, \Delta, h) = s_{\rm imp}(\alpha, \Delta, 0) - k_1(\alpha) \left(\frac{h}{T_K}\right)^2, \tag{2.4}$$

with $k_1(\alpha)$ being a known cut-off independent function. However, in this case, $s_{\rm imp}(\alpha, \Delta, 0)$ is in general non-universal and only the second term exhibits scaling. The general results are illustrated in figure 1 where $s_{\rm imp}(\alpha, \Delta = 0.01\omega_c, h)$ (E on the figure label) is plotted versus α for a range of h/ω_c. In general, $E \to 0$ for non-zero h since the field eventually will polarize the spin leading to a loss of entanglement. On the other hand, for $\alpha \to 1^-$, for $h = 0$ and $\Delta/\omega_c \to 0$, we obtain the *isotropic* $SU(2)$ Kondo model for which $\langle\sigma_x\rangle \sim \langle\sigma_z\rangle = 0$, with maximal entanglement $E \sim 1$. Hence, for $h = 0$ $s_{\rm imp}(\alpha)$ is a monotonically increasing function where as for non-zero h a maximum associated with the crossover $h \sim T_K$ occurs. The case of a sub-Ohmic heat bath has also been studied [5].

The usual Kondo Hamiltonian [45, 46] contains a Heisenberg interaction between an $s = 1/2$ impurity spin, S, and otherwise non-interacting electrons. A simple model takes a free electron dispersion relation and a δ-function Kondo interaction:

$$H = \int {\rm d}^3 r [\psi^\dagger(-\nabla^2/2m)\psi + J_K \delta^3(\vec{r})\psi^\dagger(\vec{\sigma}/2)\psi \cdot \vec{S}]. \tag{2.5}$$

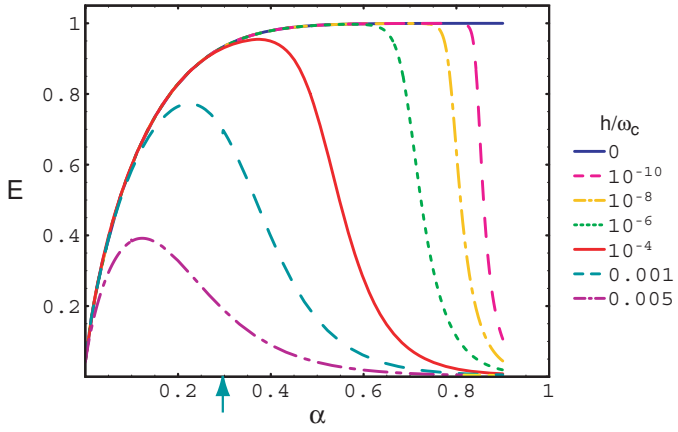

Figure 1. $s_{\rm imp}(\alpha, \Delta = 0.01\omega_c, h)$ (E on the figure label) as a function of α for a range of h/ω_c. E is defined with at $\log_2$ instead of the ln used in equations (1.1) and (2.1), resulting in a maximal entanglement of $E = 1$ *not* $E = \ln(2)$. The arrow marks the point at which $T_K = 0.001\omega_c$ [4]. Reprinted with permission from Kopp A and Le Hur K 2007 *Phys. Rev. Lett.* **98** 220401. Copyright by the American Physical Society.

(Actually, an ultra-violet cut-off of the δ-function interaction is necessary for the model to be completely well defined.) In the ground state of the Kondo model, the impurity spin is screened by the conduction electrons through the formation of a singlet. This phenomenon is expected to take place on a length scale:

$$\xi_K = v/T_K \propto e^{1/(\nu J_K)}, \tag{2.6}$$

where ν is the density of states per spin band, T_K is the Kondo scale and v is the velocity of the fermions. Due to the δ-function form of the interaction equation (2.5) can be reduced to a one-dimensional model which can be represented by a lattice model of finite extent R (including the impurity), suitable for numerical studies. As outlined above and discussed in more detail in section 3.2, we expect the case of R *odd* to reflect Kondo physics and possibly scaling with R/ξ_K. However, it has been shown [8] that $s_{\rm imp}$ exhibits weak scaling violations from the expected R/ξ_K scaling. In particular, $m_{\rm imp}$ was shown to take the form

$$m_{\rm imp} \sim \frac{1}{2} - \left[\frac{J_K}{\pi v}\right]^2 \ln(R/a), \tag{2.7}$$

where a is a short distance cutoff. Hence, weak scaling violations are present in $m_{\rm imp}$ and therefore also in $s_{\rm imp}$ even though $s_{\rm imp}$ clearly displays the expected crossover related to Kondo physics. The presence of such scaling violations is illustrated in figure 2.

Finally, recent work has focused on the entanglement between the two impurity spins in the two-impurity Kondo model [3, 7, 47, 48] including spin–orbit interactions [7], as well as the pairwise entanglement between end spins in open-ended Heisenberg spin chains [49].

3. Impurity entropies from the CFT perspective

In this section, we review the concept of thermodynamic impurity entropy and its connection with CFT. We also connect it with topological entropy in 2D topological insulators and discuss various applications of these general ideas to specific models: spin chains with boundary fields, Kondo model and point contact in a Hall bar.

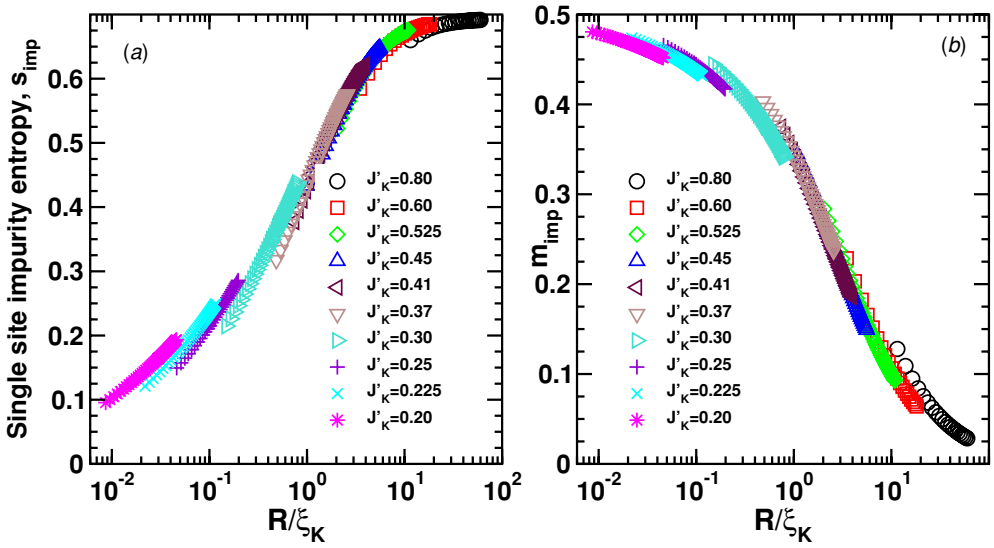

Figure 2. (*a*) Weak scaling violations for the single site impurity entanglement entropy $s_{\rm imp}$ (*a*) (equation (2.1)) and the local impurity magnetization $m_{\rm imp} = \langle S_1^z \rangle$ (*b*). Results are shown for a spin-chain model of a Kondo impurity where an impurity spin is coupled to the rest of the chain with a coupling J'_K. See section 3. All data are for odd length chains between $R = 19 \ldots 101$. Reprinted from [8]. Copyright (2007) by IOP Publishing Ltd.

3.1. Thermodynamic impurity entropy

Thermodynamic impurity entropy can be measured experimentally from impurity-specific heat using the thermodynamic identity

$$C = T\frac{\partial S}{\partial T}. \tag{3.1}$$

The impurity contribution to the specific heat, and hence the entropy, can be measured by subtracting off the same quantity for the pure system. Such measurements and related theoretical calculations have been performed for many years in Kondo impurity systems.

$C(T)$ for a metal with a dilute random array of magnetic impurities is measured and $C(T)$ for the pure system is subtracted off. Dividing by the number of impurities and extrapolating to zero impurity density gives the contribution to the specific heat of a single impurity, $C_{\rm imp}(T)$. From integrating $C_{\rm imp}(T)/T$ one can, at least in principle, obtain $S^{\rm Th}_{\rm imp}(T)$. We consider the infinite volume limit, so that $S^{\rm Th}_{\rm imp}(T)$ becomes a function of T only. We may formally define $S^{\rm Th}_{\rm imp}(T)$ by calculations on a 1D system of length R with a single impurity:

$$S^{\rm Th}_{\rm imp}(T) \equiv \lim_{R\to\infty}[S(T, R) - S_0(T, R)]. \tag{3.2}$$

Here, $S(T,R)$ is the thermodynamic entropy with the impurity present and $S_0(T, R)$ is the same quantity without the impurity. $S^{\rm Th}_{\rm imp}(T)$ exhibits interesting T-dependence which reflects the RG flow of the Kondo model. It can be calculated with high precision from the Bethe ansatz solution of the Kondo model first derived by Andrei [50] and Wiegmann [51]. In the limit of a weak bare Kondo coupling $S^{\rm Th}_{\rm imp}(T) \approx \ln 2$ at $T \gg T_K$ and $S^{\rm Th}_{\rm imp}(T) \to 0$ at $T \ll T_K$. This reflects the fact that the bare coupling of the magnetic impurity to the conduction electrons is very weak so that we obtain essentially the full entropy of a free spin-1/2, $\ln 2$ at $T \gg T_K$.

However, as the temperature is lowered, the spin is 'screened', i.e. it goes into a singlet state and the impurity entropy is accordingly lost. The asymptotic values of $S_{\rm imp}^{\rm Th}(T)$ at high and low temperatures are characteristic of the RG fixed points of the Kondo Hamiltonian.

The k-channel Kondo model

$$H = \int \mathrm{d}^3 r \sum_{i=1}^{k} [\psi^{\dagger i}(-\nabla^2/2m)\psi_i + J_K \delta^3(\vec{r})\psi^{\dagger i}(\vec{\sigma}/2)\psi_i \cdot \vec{S}] \tag{3.3}$$

also has $S_{\rm imp}^{\rm Th}(T) \approx \ln 2$ at $T \gg T_K$. However, it was found, from the Bethe ansatz solution, that at $T \to 0$ it has the limiting value $\ln g$ where [11]

$$g = 2\cos[\pi/(2+k)] \leqslant 2. \tag{3.4}$$

Heuristically, g represents a 'fractional ground state degeneracy' characterizing the non-Fermi liquid ground state of the overscreened Kondo model.

The interesting behavior of the impurity entropy in the multi-channel Kondo model was later shown to be a special case of a general phenomenon in quantum impurity models. Many models of this type have low energy descriptions in terms of 1D CFTs. Quite general boundary conditions and boundary interactions are expected to renormalize, at low energies, to CIBCs. Cardy showed that generally CIBCs can be associated with boundary states, $|A>$. The conformally invariant partition function defined on a strip of length R, at inverse temperature β, with CIBCs A and B at the two ends can be written as

$$Z^{AB} = \mathrm{tr} \mathrm{e}^{-\beta H_{AB}^R}, \tag{3.5}$$

where H_{AB}^R is the Hamiltonian on an interval of length R with BCs A and B at the two ends. Alternatively, we may switch space and imaginary time directions and write

$$Z^{AB} = \langle A|\mathrm{e}^{-RH_P^\beta}|B\rangle. \tag{3.6}$$

Now the system propagates for time R, under the action of the Hamiltonian defined on a periodic interval of length β with initial and final states $|A\rangle$ and $|B\rangle$. The boundary states can be expanded in a complete basis of Ishibashi states, $|a>$, associated with each conformal tower, a:

$$|A\rangle = \sum_a |a\rangle\langle a0|A\rangle, \tag{3.7}$$

with $|a_0\rangle$ the corresponding highest weight state. (The Ishibashi states $|a>$ are sums over all descendants with equal weight in left and right-moving sectors.) Thus, we may write

$$\begin{aligned} Z^{AB} &= \sum_a \langle A|a0\rangle\langle a0|B\rangle\langle a|\mathrm{e}^{-RH_P^\beta}|a\rangle \\ &= \sum_a \langle A|a0\rangle\langle a0|B\rangle\chi_a(\mathrm{e}^{-4\pi R/\beta}), \end{aligned} \tag{3.8}$$

where χ_a is the character of the ath conformal tower. Written in this form it is straightforward to extract the impurity entropy. Taking the limit $R \gg \beta$ only the highest weight state in the conformal tower of the identity operator contributes, giving

$$Z^{AB} \to \mathrm{e}^{\pi Rc/6\beta}\langle A|00\rangle\langle 00|B\rangle. \tag{3.9}$$

(Here c is the central charge associated with the bulk CFT.) From this expression we obtain the entropy

$$S^{\rm AB,Th} = \frac{\partial}{\partial T}[T \ln Z^{AB}] = \frac{\pi RcT}{3} + \ln g^{AB}, \tag{3.10}$$

where

$$g^{AB} = g^A \cdot g^B = \langle A|00\rangle\langle 00|B\rangle. \tag{3.11}$$

This consists of the bulk term, independent of the boundary conditions and proportional to the system size, R, as well as the boundary term $\ln g$ which is a sum of contributions from each boundary. Using the known boundary state corresponding to the non-Fermi liquid ground state of the multi-channel Kondo model, we can re-obtain the Bethe ansatz result for $S_{\rm imp}^{\rm Th}(T=0)$ from this general CFT formula.

$\ln g$, the $T = 0$ thermodymamic entropy, is a universal property of fixed points of the boundary RG. It has the interesting property that it always *decreases* under RG flow from an unstable to stable fixed point [11, 52]. Equation (3.4) provides an example of this: the impurity entropy is $\ln 2$ at the unstable fixed point, $T \gg T_K$, and always has a smaller value at the stable fixed point which occurs at $T = 0$.

3.2. Boundary term in the entanglement entropy

We now consider a semi-infinite CFT ($r \geqslant 0$) with CIBC, of type A at $r = 0$. We consider the ground state entanglement entropy for the region, $0 \leqslant r' \leqslant r$, $S^A(r)$. The entanglement entropy has been shown to be [13–15, 12]

$$S^A(r) = \frac{c}{6}\ln\left(\frac{r}{a}\right) + c^A + \frac{s_1}{2}. \tag{3.12}$$

For a review, see the article by Calabrese and Cardy in this series [39]. We can argue that $c^A = \ln g^A$, the thermodynamic impurity entropy, by the device of considering the entanglement entropy for this system at finite temperature. C&C [12] showed that the generalization of $S^A(r)$ to a finite inverse temperature, β, is given by a standard conformal transformation:

$$S^A(r,\beta) = \frac{c}{6}\ln\left[\frac{\beta}{\pi a}\sinh\left(\frac{2\pi r}{\beta}\right)\right] + c^A + s_1/2. \tag{3.13}$$

See also [15]. $S^A(r,\beta)$ is defined by beginning with the Gibbs density matrix for the entire system, $\mathrm{e}^{-\beta H}$ and then again tracing out the region $r' > r$. Now consider the high temperature, long length limit, $\beta \ll r$:

$$S^A \to \frac{2\pi cr}{6\beta} + \frac{c}{6}\ln\left(\frac{\beta}{2\pi a}\right) + c^A + \frac{s_1}{2} + O(\mathrm{e}^{-4\pi r/\beta}). \tag{3.14}$$

The first term is the extensive term (proportional to r) in the thermodynamic entropy for the region, $0 < r' < r$. The reason that we recover the thermodynamic entropy when $r \gg \beta$ is because, in this limit, we may regard the region $r' > r$ as an 'additional reservoir' for the region $0 \leqslant r' \leqslant r$. That is, the thermal density matrix can be defined by integrating out degrees of freedom in a thermal reservoir, which is weakly coupled to the entire system. On the other hand, the region $r' > r$ is quite strongly coupled to the region $r' < r$. Although this coupling is quite strong, it only occurs at one point, r. When $r \gg \beta$, this coupling only weakly perturbs the density matrix for the region $r' < r$. Only low energy states, with energies of order $1/r$ and a negligible fraction of the higher energy states (those localized near $r' = r$) are affected by the coupling to the region $r' > r$. The thermal entropy for the system, with the boundary at $r = 0$ in the limit $r \gg \beta$, is

$$S^{\rm A,Th} \to \frac{2\pi cr}{6\beta} + \ln g^A + \text{constant}, \tag{3.15}$$

with corrections that are exponentially small in r/β. The only dependence on the CIBC, in this limit, is through the constant term, $\ln g^A$, the impurity entropy. Thus, it is natural to

identify the BC-dependent term in the entanglement entropy with the BC-dependent term in the thermodynamic entropy:

$$c^A = \ln g^A. \tag{3.16}$$

This follows since, in the limit, $r \gg \beta$, we do not expect the coupling to the region $r' > r$ to affect the entanglement entropy associated with the boundary $r' = 0$, c^A. Note that the entanglement entropy, equation (3.14), contains an additional large term not present in the thermal entropy. We may ascribe this term to a residual effect of the strong coupling to the region $r' > r$ on the reduced density matrix. However, this extra term does not depend on the CIBC as we would expect in the limit $r \gg \beta$ in which the 'additional reservoir' is far from the boundary. Now passing to the opposite limit $\beta \to \infty$, we obtain the remarkable result that the only term in the (zero temperature) entanglement entropy depending on the BC is precisely the impurity entropy, $\ln g^A$, equation (1.2). We may also consider a finite system, of length R, with ICBC at both ends. In the case, where both BCs are the same, A, we expect the generalization of equation (1.2) which follows from a conformal transformation:

$$S^A(r, R) = \frac{c}{6} \ln \left[\frac{2R}{\pi a} \sin \left(\frac{\pi r}{R} \right) \right] + \ln g^A + \frac{s_1}{2}, \tag{3.17}$$

with the equivalent result for periodic boundary conditions:

$$S^{\mathrm{A,PBC}}(r, R) = \frac{c}{3} \ln \left[\frac{R}{\pi a} \sin \left(\frac{\pi r}{R} \right) \right] + s_1. \tag{3.18}$$

As usual, a denotes the lattice spacing. A result has not been obtained, as far as we know, for the case where the CIBCs are different at the two ends.

As discussed in the previous subsection, the thermodynamic impurity entropy, $\ln g$, is a universal quantity with interesting RG behavior. It is then natural to expect that the impurity term in the entanglement entropy will behave similarly. In particular, consider beginning with a CFT on the semi-infinite line with CIBC A and then adding a small relevant boundary interaction

$$H = H_{\mathrm{CFT}} - \lambda \phi(0), \tag{3.19}$$

where ϕ has an RG scaling dimension $y < 1$. ($y = 1$ is the marginal dimension for *boundary* interactions, since the action contains only a time integral over $\phi(\tau, r = 0)$ and no spatial integral.) We expect that, under the renormalization group, the Hamiltonian will flow to an infrared stable fixed point, at long length scales, characterized by some other CIBC, B. The 'g-theorem' [11, 52] implies that the thermodynamic impurity entropy at the stable fixed point obeys $g^B < g^A$. Typically the flow between fixed points can be controlled by introducing a finite length scale which acts as an infrared cutoff. This is often done by putting the system in a finite box, of size R. It is not obvious what will happen when we have no physical box but introduce a length scale l by the definition of the entanglement entropy. Will the impurity part of the entanglement entropy exhibit a crossover from g^A to g^B as we increase l? Will this cross over be universal? These questions have been investigated numerically, using the DMRG method, in a couple of models.

3.2.1. The transverse field Ising model. The first model considered was the 1D transverse field Ising model with a longitudinal boundary magnetic field [16]:

$$H = -\sum_{j=0}^{L-1} \left(S_j^z S_{j+1}^z + (1/2) S_j^x \right) + h_b S_0^z + h_b S_L^z. \tag{3.20}$$

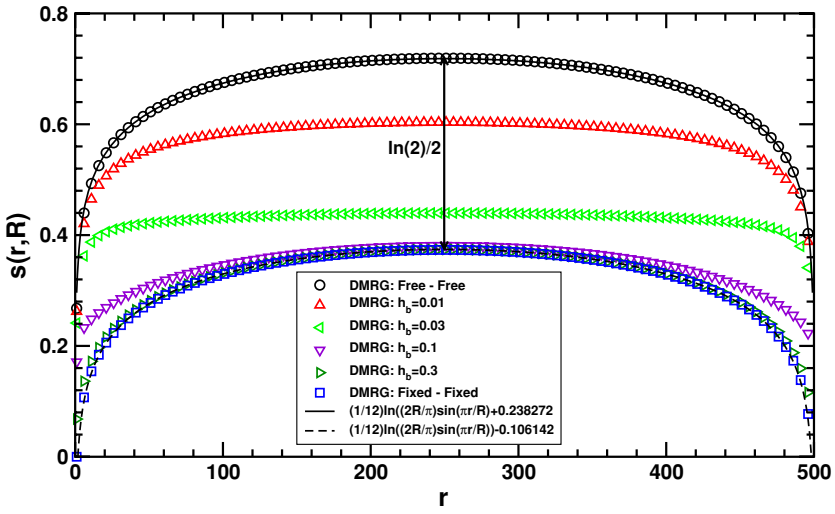

Figure 3. $S(r, R)$ versus r ($R = 500$) for the transverse field Ising model calculated using DMRG with $m = 128$. Results are shown for free–free and fixed–fixed boundary conditions along with four different values of $h_b = 0.01, 0.03, 0.10, 0.30$. For the numerical DMRG data only every fourth point is shown for clarity. The solid and dashed lines represent fits of the DMRG results for free–free and fixed–fixed BCs, respectively, to the analytical result equation (3.17). For the latter case, calculations were performed formally with $h_b = \infty$.

The bulk transverse field has been tuned to its critical value, $1/2$. A weak longitudinal field, h_b is applied at the boundaries, $j = 0, L$, only. This boundary field is relevant, with dimension 1/2 and therefore induces a boundary RG flow between the only two boundary-fixed points in this model, corresponding to free or fixed BC. The values of g are $g = 1$ (free) and $g = 1/\sqrt{2}$ (fixed). DMRG results on chains of length up to 800, keeping 140 block states, showed quite convincingly that the entanglement entropy crosses over from $(1/12)\ln(r/a)$ to $(1/12)\ln(r/a) - (1/2)\ln 2$ as r is increased from small values to values larger than a crossover scale, ξ, determined by h_b as $\xi \propto |h_b|^{-1/2}$. In figure 3 we illustrate these results by calculations on systems with $R = 500$. In figure 4, we also show the entanglement entropy with *different* BCs at the ends of a finite chain, fixed–free and fixed up–fixed down. As far as we know, no analytic formulas have been derived for these cases. We note that the expression

$$S(r, R) = \frac{1}{12}\ln\left[\frac{R}{a}\sin\left(\frac{\pi r}{R}\right)\right] - \ln\left[\cos\left(\frac{\pi r}{4R}\right)\right] + \text{constant} \tag{3.21}$$

seems to fit the data quite well in the fixed–free case.

3.2.2. The Kondo model. The second model in which this crossover was studied is the Kondo model [8, 17]. For this model, we may consider the entanglement of a region inside a sphere of size r surrounding the impurity, with the rest of space which may either be infinite or confined to a larger sphere of size R. The impurity entanglement entropy is defined as the increase in entanglement arising when the impurity is added to the system. This mimics the definition of the impurity thermodynamic entropy which has been well studied experimentally and theoretically for Kondo systems. Due the δ-function form of the Kondo interaction, the 3D model is equivalent to a 1D model. To see this, we expand the electron fields in spherical harmonics. Only the s-wave interacts with the impurity spin, the other harmonics being

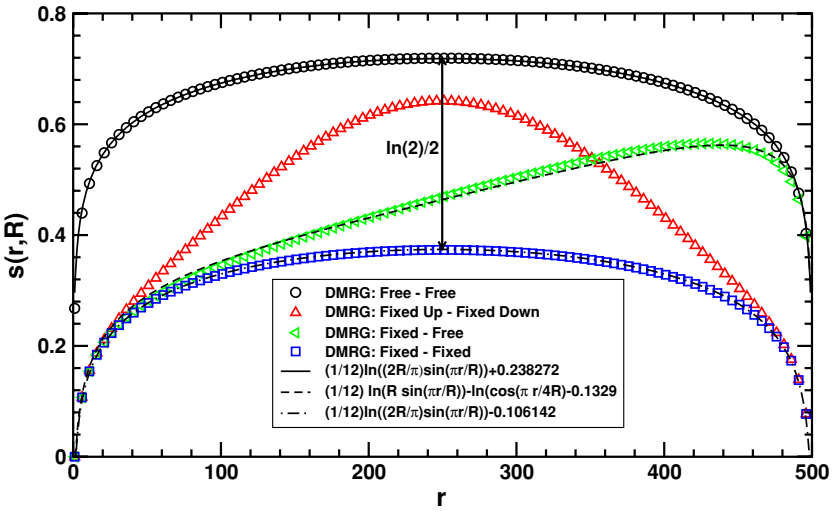

Figure 4. $S(r, R)$ versus r ($R = 500$) for the transverse field Ising model calculated using DMRG with $m = 128$. Results are shown for free–free and fixed–fixed boundary conditions along with free–fixed and fixed (up)–fixed (down) boundary conditions. For the numerical DMRG data only every fourth point is shown for clarity. The solid and dashed lines represents fits of the DMRG data for free–free and fixed–fixed BCs, respectively, to the analytical result equation (3.17). The calculations with fixed boundaries are performed by formally setting $h_b = \pm\infty$.

completely free. The entanglement entropy may be written as a sum of contributions from each spherical harmonic:

$$S = \sum_{l,m} S_{l,m}. \tag{3.22}$$

Only the s-wave part, $S_{0,0}$ is affected by the Kondo interaction so that the total impurity entanglement entropy is given by the change in $S_{0,0}$ when the impurity spin is added. Assuming that the Kondo coupling is weak, as is usually the case in experiments, we may integrate out Fourier components of the s-wave electron fields except for a narrow band around the Fermi sphere. Linearizing the dispersion relation near the Fermi energy:

$$k^2/2m \approx k_F^2/2m + v_F(k - k_F), \tag{3.23}$$

the model becomes equivalent to a relativistic Dirac fermion defined on the half-line, $r > 0$ interacting with the impurity spin at $r = 0$:

$$H_{1D} \approx (\mathrm{i}v_F/2\pi)\int_0^R \mathrm{d}r[\psi_L^\dagger(\mathrm{d}/\mathrm{d}r)\psi_L - \psi_R^\dagger(\mathrm{d}/\mathrm{d}r)\psi_R] + v_F\lambda_K\psi_L^\dagger(0)(\vec{\sigma}/2)\psi_L(0)\cdot\vec{S}. \tag{3.24}$$

Here $\lambda_K \propto J$ and a boundary condition

$$\psi_L(0) = -\psi_R(0) \tag{3.25}$$

is imposed on the left and right movers.

To obtain a model amenable to DMRG studies, we could consider a 1D tight-binding version of this 1D continuum model. However, considerable numerical speed-up can be obtained by considering a 'spin-only' version of the model. This is based on spin-charge

separation for 1D interacting fermion systems, which follows from bosonization. We find that only the spin degrees of freedom of the 1D electrons interact with the impurity, *when it is at the end of the chain*. (Things are more complicated when it is not at the end. The simplifications at the end arise from the BC of equation (3.25).) The spin part of the Hamiltonian, the only part involving the Kondo interaction, can be written as a perturbed $SU(2)_1$ Wess–Zumino–Witten nonlinear σ-model with Hamiltonian

$$H_s = (v_F/2\pi)\int_0^R \mathrm{d}r(1/3)[\vec{J}_L\cdot\vec{J}_L + \vec{J}_R\cdot\vec{J}_R] + v_F\lambda_K\vec{J}_L(0)\cdot\vec{S}. \tag{3.26}$$

Here $\vec{J}_{L/R}(r)$ are the spin density operators for left and right movers, with the BC

$$\vec{J}_L(0) = \vec{J}_R(0). \tag{3.27}$$

This implies that we may regard $\vec{J}_R(r)$ as the analytic continuation of $J_L(r)$ to the negative r axis:

$$J_R(r) = \vec{J}_L(-r) \tag{3.28}$$

and write the theory in terms of left movers only defined on the interval $-R < r < R$:

$$H_s = (v/6\pi)\int_{-R}^R \mathrm{d}r\vec{J}_L\cdot\vec{J}_L + v_F\lambda_K\vec{J}_L(0)\cdot\vec{S}. \tag{3.29}$$

Now consider Heisenberg antiferromagnetic $S = 1/2$ chain with one weak link at the end:

$$H = J_K'\vec{S}_1\cdot\vec{S}_2 + \sum_{r=2}^{R-1}\vec{S}_r\cdot\vec{S}_{r+1}. \tag{3.30}$$

For $J_K' \ll 1$ essentially the same low energy continuum limit field theory, equation (3.26) is obtained except that the Fermi velocity, v_F, is replaced by the spin-velocity, which we call v. This model is considerably more efficient to study with DMRG since there are only two states per site rather than four. Actually, a drawback of this model is that there is an important marginally irrelevant bulk interaction in the low energy Hamiltonian

$$\delta H = -(gv/2\pi)\vec{J}_L\cdot\vec{J}_R, \tag{3.31}$$

with the positive dimensionless coupling constant g of $O(1)$. This leads to logarithmically varying corrections to all quantities which greatly hinders numerical work. To circumvent this problem, it is advantageous to add a second neighbor interaction, considering instead the Hamiltonian

$$H = J_K'(\vec{S}_1\cdot\vec{S}_2 + J_2\vec{S}_1\cdot\vec{S}_3) + \sum_{r=2}^{R-1}\vec{S}_r\cdot\vec{S}_{r+1} + J_2\sum_{r=2}^{R-2}\vec{S}_r\cdot\vec{S}_{r+2}. \tag{3.32}$$

For $J_2 > J_2^c \approx 0.2412$, the model goes into a gapped dimerized phase, of which the exactly solvable Majumdar–Ghosh model with $J_2 = 1/2$ is a special simple case. The gap is driven by the marginal coupling constant g which changes sign at J_c^c, becoming marginally relevant. For $J_2 < J_2^c$, the model remains gapless with the marginal coupling constant g and the spin velocity v varying smoothly. Right at the critical point, $J_2 = J_2^c$, $g = 0$. At this point, all logarithmic corrections vanish and it becomes possible to extract meaningful results from numerical studies of relatively short chains. Therefore, we largely focussed on this $J_2 = J_2^c$ model. As discussed in more detail in [53] and references therein, we then see that the low energy effective field theory description of the spin-only model, equation (3.32), with $J_2 = J_2^c$ ($g = 0$) is *the same* as that of the usual electronic version of the Kondo model.

As summarized in subsection 3.1, the thermodynamic impurity entropy, $S_{\mathrm{imp}}^{\mathrm{Th}}(T)$, decreases monotonically from $\approx \ln 2$ at $T \gg T_K$ to zero at $T \ll T_K$. We might expect

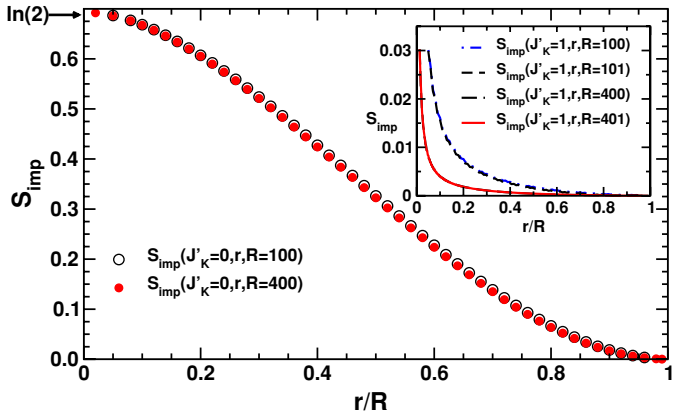

Figure 5. DMRG results using spin inversion with $m = 256$ for $S_{\rm imp}(0, r, R)$ for $\mathcal{R}$ even ($R = 100, 400$). Results are shown for the $J_1 - J_2$ spin-chain model at J_2^c. Inset: DMRG results for $S_{\rm imp}(1, r, R)$ for R odd and even. Data for $R = 100, 101$ and $R = 400, 401$ are indistinguishable. $S_{\rm imp}(1, r, R)$ appears to vanish in the scaling limit $r \to \infty$ with r/R held fixed.

that the impurity entanglement entropy would behave the same same with the energy scale, T replaced by v/r where r is the size of the region A. While we ultimately confirmed this result, two interesting subtleties were encountered *en route*.

First of all, even for an infinite system size, R, we found that the entanglement entropy has an alternating term, $S_{\rm A}$, which decays only slowly with r [23]:

$$S(r, R) = S_{\rm U}(J'_K, r, R) + (-1)^r S_{\rm A}(J'_K, r, R), \tag{3.33}$$

We discuss this in section 5. Note that we use a lower subscript $S_{\rm A}$ to denote the alternating part of the entanglement entropy to distinguish it from $S^{\rm A}$, the entanglement entropy with CIBC A. Although we expect $S_{\rm U}$ to be essentially the same in the spin-chain Kondo model as in the fermion Kondo model, the same is not true of $S_{\rm A}$. (More generally, the fermion model is expected to have a term in the entanglement entropy oscillating at the wave-vector $2k_F$.) Henceforth, in this section, we focus on the uniform part, $S_{\rm U}$ only.

We extracted an impurity part from $S_{\rm U}$ by

$$S_{\rm imp}(J'_K, r, R) \equiv S_{\rm U}(J'_K, r, R) - S_{\rm U}(1, r-1, R-1), \ r > 1. \tag{3.34}$$

Note that we are subtracting the entanglement entropy of a chain where all couplings have unit strength and one site is removed. This corresponds to subtracting the entanglement entropy of the system without the impurity. It is important here that we do not subtract the entropy for the same values of r and R but with $J'_K = 0$ since, as we discuss below, entanglement with the impurity can survive, even in this limit, when R is even, in the spin-singlet ground state (see figure 5). This is related to the second subtlety that we encountered: a very strong dependence of $S_{\rm imp}$, as defined by equation (3.34), on the parity of R, even after subtracting off the part alternating in r. This is illustrated by some of our DMRG data shown in figure 6.

This figure tests the conjecture that the impurity entanglement entropy shows universal RG scaling behavior. We find that the data for the impurity entanglement entropy for various Kondo couplings can be collapsed onto scaling curves which depend only on the dimensionless ratios r/ξ_K, where ξ_K is the Kondo length scale, and r/R. However, there are two different sets of curves depending on the parity of R. Note that the curves differ markedly for $r \ll \xi_K$ but elsewhere look similar. Indeed it looks likely, and presumably must be the case, that as

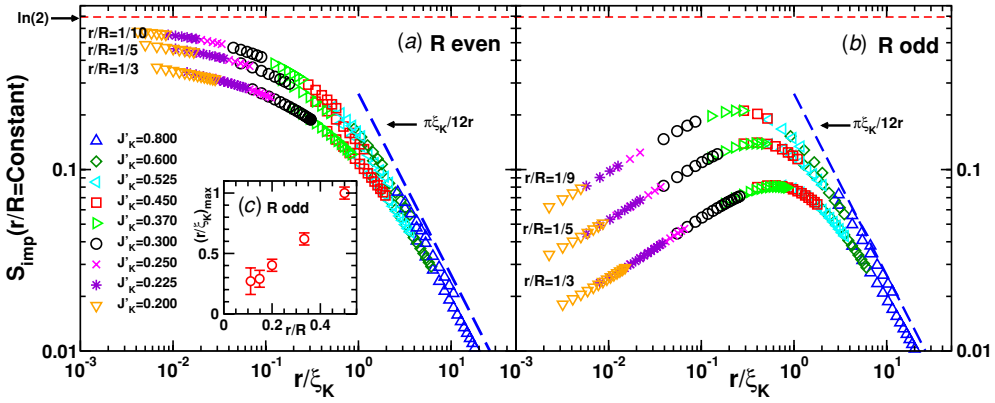

Figure 6. Universal scaling plot of $S_{\rm imp}$ for fixed r/R, (*a*) for $R \leqslant 102$ *even*, (*b*) for $R \leqslant 101$ *odd*. DMRG results with $m = 256$ for the $J_1 - J_2$ chain at J_2^c for various couplings J_K'. The lines marked $\pi\xi_K/(12r)$ are the FLT prediction: equation (3.39). (*c*) The location of the maximum, $(r/\xi_K)_{\rm max}$, of $S_{\rm imp}$ for odd R, plotted versus r/R. Reprinted from [8]. Copyright (2007) by IOP Publishing Ltd.

$r/R \to 0$, the curves become identical for even and odd R. Focusing on the even R curves, which seem close to the $r/R \to 0$ limit, the scaling curves seem to approach a monotone decreasing function with the value $\ln 2$ at $r \ll \xi_K$ and zero for $r \gg \xi_K$. This is exactly what we would expect from the RG theory of the Kondo model and mirrors the T-dependence of the thermodynamic impurity entropy, reviewed in subsection 3.1. In particular, $\ln g = \ln 2$ at the short distance weak coupling fixed point, corresponding to a paramagnetic spin-1/2 impurity but $\ln g = 0$ at the long distance strong coupling fixed point, corresponding to the spin being screened.

A qualitative understanding of the surprising difference between even and odd R can be obtained using a 'resonating valence bond' picture of the ground state of the $s = 1/2$ Heisenberg antiferromagnetic chain [8]. Consider first even R. Any singlet state can be written as a linear superposition of products of singlet states formed by pairs of spins. Conventionally one draws a line or 'valence bond' between pairs of spins contracted to a singlet, $(|\uparrow\downarrow> - |\downarrow\uparrow>)/\sqrt{2}$. It can easily be shown that by restricting to terms in which none of the lines cross, we get a complete linearly independent set of singlet states for an $S = 1/2$ chain. Furthermore, by adopting a convenient sign convention for valence bond states, it can be proven that all terms in the sum have non-negative coefficients. We may heuristically associate the impurity entanglement entropy with the valence bond originating from the impurity spin at site 1. If this spin forms a singlet with a spin at a site inside region A (at a site with index $\leqslant r$), then we consider this not to contribute to the impurity entanglement entropy, $S_{\rm imp}$ of region A. On the other hand, if site 1 is paired with a site outside region A (with index $> r$) then we consider it to contribute to $S_{\rm imp}$. The ground state is a sum over many valence bond configurations so we could imagine relating $S_{\rm imp}$ to the probability of this 'impurity valence bond' (IVB) extending out of region A [8, 17]. (See figure 7) Similar ideas have been explored in [54]. As J_K' gets smaller, the IVB gets longer ranged. This follows because, in general, valence bonds tend to be the nearest neighbor, or at least quite short range in order to take advantage of the nearest-neighbor antiferromagnetic interactions. However, as J_K' gets weaker there is less and less energetic advantage in a short impurity valence bond. In the extreme case $J_K' = 0$ the impurity valence bond extends with significant probability over the entire chain. We expect that the typical length of this impurity valence bond should

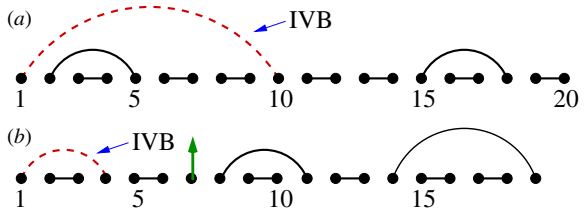

Figure 7. Typical impurity valence bond configurations for R even (a) and R odd (b). Note the unpaired spin on the seventh site in (b). Reprinted from [8]. Copyright by IOP Publishing Ltd.

be ξ_K, the Kondo screening cloud size. This is a characteristic length scale, of order v/T_K, at which the effective Kondo coupling becomes of order 1. In a metal, one heuristically imagines an electron in a quasi-bound state forming a singlet with the impurity spin with ξ_K being the extent of the bound state wavefunction. In the spin-chain realization of the Kondo model, this quasi bound state corresponds to the impurity valence bond. Thus, the fact that $S_{\rm imp}$ starts to decrease when r exceeds ξ_K is very natural from this Kondo screening cloud viewpoint. Unfortunately, it seems extremely difficult to make this more than a heuristic argument. A problem is that the valence bond basis, while complete and linearly independent, is not an orthonormal basis. Although one could define a probability distribution for the length of the IVB, it is hard to relate this to physical quantities such as the correlation length or the entanglement entropy. However, we can formally write

$$S_{\rm imp}^{\rm IVB} = (1-p)\ln 2, \tag{3.35}$$

with p the probability that the IVB connects the impurity spin to a spin in region A. This follows, since if the IVB does *not* cross the boundary between regions A and B its contribution to $S_{\rm imp}$ is obviously zero, and on the other hand, if the IVB connects to a spin in region B it will contribute a factor of $\ln(2)$. It is possible to be a little bit more quantitative using the recently introduced valence bond entropy [55, 56]. If one simply focuses on the IVB connecting the spin impurity with the rest of the system, we expect the probability $\mathcal{P}$ that the IVB has a length r to decay like ξ_K/r^2 in the regime $r \gg \xi_K$, thus giving

$$S_{\rm imp}^{\rm IVB}(r) = \ln 2\left(1 - \int_1^r \mathcal{P}\mathrm{d}r'\right) \sim A\ln(2)\frac{\xi_K}{r}(r \gg \xi_K). \tag{3.36}$$

Such a $1/r^2$ behavior is expected for a pure system [57].

Now consider the case of odd R. The ground state now has a total spin of 1/2. We may again represent it by valence bonds but there are $(R-1)/2$ of them with one unpaired spin. This unpaired spin may or may not be the impurity spin. As J_K' gets weaker it becomes more and more likely that the impurity spin is unpaired. Clearly when $J_K' = 0$ the other $R-1$ spins form a singlet leaving the impurity in a paramagnetic state. In this limit, for odd R, $S_{\rm imp}$ is precisely zero, due to the way we have defined it. Numerically, we find that the maximum in $S_{\rm imp}$, for odd R, occurs at a value of J_K' such that $\xi_K \propto R/2$. This is due to the trade-off between two competing effects. As we decrease ξ_K from large values, we increase the probability of having an IVB (i.e. of the impurity not being the unpaired spin). This tends to increase $S_{\rm imp}$. However, once ξ_K becomes less than R, the shortening of the IVB with decreasing ξ_K becomes important and decreases $S_{\rm imp}$. It is now clear that the limits $\xi_K \to \infty$ and $R \to \infty$ do not commute. Taking $R \to \infty$ for any fixed r and ξ_K gives the same $S_{\rm imp}(r/\xi_K)$ as occurs for even R: a monotone decreasing function. However, holding R fixed and varying ξ_K gives a maximum of $S_{\rm imp}$ in the vicinity of $\xi_K \approx R$. Again, this is largely a heuristic picture.

While we so far only have heuristic descriptions of $S_{\rm imp}$ when ξ_K is of order R and/or r, CFT methods can be used to calculate an analytic expression for $S_{\rm imp}$ in the opposite limit $\xi_K \ll r$ (for any ratio of r/R) [8, 17]. (Note that in this limit the dependence on the parity of R disappears.) This calculation is based on doing perturbation theory for $S_{\rm imp}$ in the leading irrelevant operator at the strong coupling, infrared fixed point. In fact such perturbation theory is very powerful and very well known for the Kondo effect, going under the name of Nozières local Fermi liquid theory (FLT). It has been used long ago to calculate the leading dependence at low temperature of thermodynamic and transport quantities. This approach can be based on the continuum limit field theory of equation (3.26). The infrared stable, strong coupling fixed point Hamiltonian does not contain the impurity spin since it is screened and breaking this singlet costs an energy of $O(T_K)$. The low energy Hamiltonian at energy scales $\ll T_K$ only contains the continuum WZW fields. In this simple, spin-only model, the only effect of the Kondo interaction, once it has renormalized to strong coupling, is to switch the finite size spectrum of the WZW model between the $s = 0$ and $s = 1/2$ conformal tower, corresponding to removing one site. To perturb around this fixed point we must identify the leading irrelevant operator which we expect to appear as a boundary interaction at $r = 0$ only. (It must be understood that this low energy theory is only valid at length scales large compared to ξ_K. We may think of the boundary interaction as being smeared over a distance of $O(\xi_K)$ but this is effectively the same as being right at the boundary, $r = 0$ in the effective Hamiltonian.) The leading irrelevant boundary operator, which must have $SU(2)$ symmetry, is simply $\vec{J}_L^2(r = 0)$. (Recall that the BC $\vec{J}_L(0) = \vec{J}_R(0)$ means there is only one boundary current operator.) Very fortunately, this leading irrelevant interaction is proportional to the bulk energy density, as we see from equation (3.29). Defining this energy density

$$\mathcal{H}_{s,L}(r) = (v/6\pi)\vec{J}_L \cdot \vec{J}_L, \tag{3.37}$$

the leading irrelevant interaction at the infrared stable fixed point is conventionally written:

$$H_{\rm int} = -(\pi\xi_K)\mathcal{H}_{s,L}(0). \tag{3.38}$$

This can be taken as a precise definition of the crossover length scale ξ_K. The fact that $H_{\rm int}$ can be written in terms of $\mathcal{H}_{s,L}$ is very convenient for calculating the leading perturbation to the entanglement entropy because we may simply takeover the earlier results of Calabrese and Cardy [12]. These imply the leading correction [17]

$$S_{\rm imp} \to \pi\xi_K/(12r), \tag{3.39}$$

representing first-order perturbation theory in ξ_K, valid when $r \gg \xi_K$. This result is obtained for infinite R but we may obtain the finite R result by a standard conformal transformation:

$$S_{\rm imp} = \frac{\pi\xi_K}{12R}\left[1 + \pi\left(1 - \frac{r}{R}\right)\cot\left(\frac{\pi r}{R}\right)\right]. \tag{3.40}$$

We find that this formula fits our numerical data, for both even and odd R, extremely well as illustrated in figure 8. Note that there are essentially no free parameters in the fit except for ξ_K which can be determined independently as a function of J_K' and is expected to behave exponentially at weak coupling:

$$\xi_K \propto \exp[1.38/J_K']. \tag{3.41}$$

(The parameter 1.38 is *not* a fitting parameter but is rather determined from a careful mapping of the weak coupling of the end spin to the Kondo coupling in the usual fermion Kondo model.) This good fit of the CFT predictions to DMRG results on the spin-chain version of the Kondo model is rather striking confirmation of the universality of entanglement entropy.

Recent work on entanglement in Kondo systems have focused on the time evolution of the entanglement [33] as well as using different measures of the entanglement to detect the Kondo screening cloud [34].

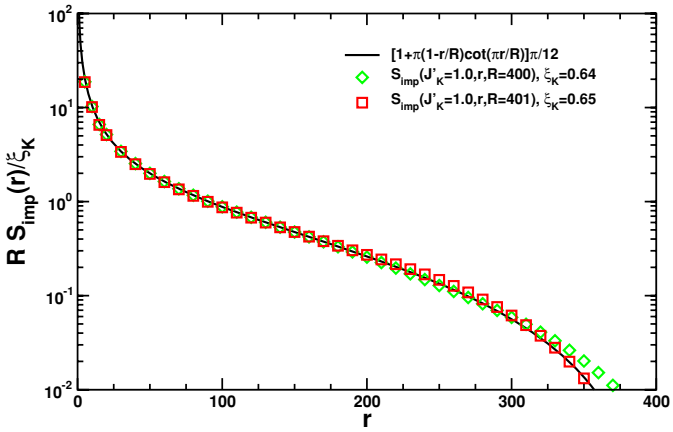

Figure 8. DMRG results with $m = 256$ for the $J_1 - J_2$ chain. $S_{\rm imp}(J'_K = 1, r, R)$ for $R = 400, 401$ with $J_2 = J_2^c$ compared to the FLT prediction, equation (3.40).

3.3. Topological entanglement entropy

We now consider a class of gapped 2D systems known as topological insulators. These occur most famously as models for the fractional quantum Hall effect although other experimentally relevant possibilities have been conjectured. The gapped excitations of these systems can exhibit non-Abelian statistics and are currently of great interest as possible topological quantum computers. It is rather difficult to demonstrate numerically that a given microscopic model has a topological ground state of a given type. Recently, it was observed that this information can be extracted from the entanglement entropy. If we consider the entanglement entropy of a finite region inside a 2D insulator of infinite extent, then we expect 'area law' behavior:

$$S = \alpha R', \tag{3.42}$$

where R' is the length of the perimeter of the region and α is a non-universal constant. However, it was recently shown [18, 19] that there is a sub-leading universal topological term in the entanglement entropy which is independent of the length and shape of the perimeter:

$$S = \alpha R' - \ln \mathcal{D}. \tag{3.43}$$

To actually extract this term, it was proposed to divide the infinite 2D space into three or four imaginary finite regions and one infinite region and to calculate a sum and difference of various entanglement entropies so that the term $\propto R$ cancels. The connection of this term with the impurity entropy $\ln g$ was suggested in [18] (see also [19]). It was further elucidated in [58] using the connection of a 2D topological insulator with a 1D edge model [59–62]. Consider for example a 'quantum Hall bar', a macroscopic sample of a topological insulator with edges. It is known that the electric current responsible for the Hall conductivity, σ_{xy}, flows around the edges only, in a clean sample, in a direction determined by the magnetic field direction, which is perpendicular to the plane. The low energy excitations on the edge correspond to a chiral CFT, meaning that the excitations are moving in only one direction. By considering a long thin Hall bar, such as in figure 9 one can formally group together the right moving excitations on the upper edge and the left moving excitations on the lower edge to obtain a parity symmetric CFT. (As in all CFTs the left and right moving sectors are decoupled.) This is a particularly convenient formulation if a constriction is created in the Hall bar, corresponding to a narrowing of the bar (usually imposed with gate voltages) at

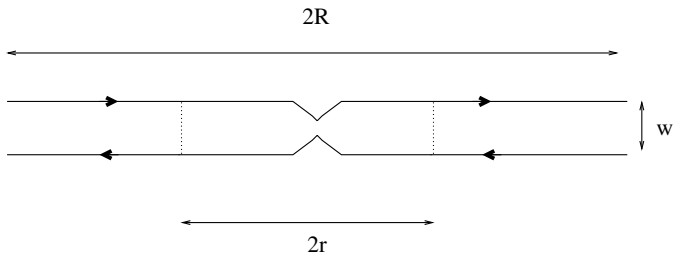

Figure 9. A long thin Hall bar with a chiral edge current and a constriction. In subsection 3.3, we let $R \to \infty$ and consider the entanglement entropy for the region of width $2r$ with the rest of the Hall bar. In subsection 3.4, we take R finite and consider the entanglement of the left side of the entire system with the right side.

one point, as shown in figure 9. The constriction leads to 'back-scattering', i.e. reflection of right-movers approaching the constriction on the upper edge into left-movers leaving it on the lower edge. Integrating out the gapped bulk modes, this can be described by a purely 1D parity symmetric field theory: a CFT with a local back-scattering interaction. In some situations, for example a simple CFT corresponding to spinless fermions with repulsive interactions, this back-scattering is a relevant interaction and can block all transport between left and right sides of the 1D system at low energies and long lengths. (This can be understood in terms of the boundary RG discussed in subsection 2.1). To make this connection more explicit let us consider the case where the constriction has zero width in the x-direction and is parity invariant so that it acts only on the parity even channel of excitations. It is then possible to make a 'folding transformation' mapping the 1D infinite system to a 1D semi-infinite system, $r \geqslant 0$ with the scatterer at $r = 0$. The incoming parity even excitations are mapped to left movers and the outgoing parity even excitations to right movers. The back-scattering interaction becomes a boundary sine-Gordon interaction for the boson field corresponding to the parity even excitations. When the back-scattering is relevant it leads to an RG flow from Neumann to Dirichlet BCs on the parity even boson. This is associated with a non-zero change in the impurity thermodynamic entropy, $\ln g$ which depends on the strength of the bulk excitations. In the original 2D model, we may think of the relevant constriction as effectively breaking the Hall bar into two pieces, each with its own chiral edge modes, as shown in figure 9.

Again we may relate the impurity thermodynamic entropy to the impurity entanglement entropy. To do this, in the original 2D model, it is convenient to consider the entanglement of some region, A, containing the constriction and extending a distance r on either side of it, with the rest of the infinite Hall bar. The corresponding entanglement entropy, in the 1D folded formulation can be decomposed into a sum of contributions from even and odd parity modes. Only the even parity part is affected by the constriction. The corresponding entanglement entropy for the even parity edge modes is

$$S = \frac{1}{3} \ln \left(\frac{r}{a} \right) + \ln g + s_1, \tag{3.44}$$

the standard result for a finite region in a semi-infinite CFT with $c = 1$ (e.g. with periodic BCs). Note that we have so far only considered the entanglement between region A and the rest due to the gapless edge modes. We expect additional contributions from the bulk modes, $2\alpha w$, where w is the width of the Hall bar and hence $2w$ is the length of the boundary of region A. Note that the extra term $(1/3) \ln r$ does not occur in the formulation of [18, 19]

where the region A does not include any physical boundaries and hence does not include any edge states.

Now consider the change in entanglement entropy for region A with the rest, as we increase the length, $2r$, of region A. We then expect an RG flow from the clean Hall bar at small r to a Hall bar broken into two at large r, with the crossover length scale determined by the strength of the back-scattering [63–66]. From the viewpoint of the low energy 1D model, the change results from the RG flow of the BC and is given by the change in $\ln g$:

$$S_{\mathrm{IR}} - S_{\mathrm{UV}} = \ln g_{\mathrm{IR}} - \ln g_{\mathrm{UV}}. \tag{3.45}$$

(Note, in particular, that the $(1/3)\ln r$ term is the same in either perfectly transmitting or perfectly reflecting limits. In the first case it is the bulk 1D entanglement entropy for a region of length $2r$ in an infinite system. In the second, it is twice the entanglement entropy for a region of length r in a semi-infinite system.) On the other hand, from the viewpoint of topological entropy, the constriction has broken the Hall bar into two pieces, without affecting the length of the perimeter, separating region A from the rest, $2w$. This is expected to double the topological entropy:

$$S_{\mathrm{IR}} - S_{\mathrm{UV}} = -\ln \mathcal{D}, \tag{3.46}$$

since, in the infrared limit, we simply get twice the entanglement entropy of the Hall bar in the region $0 < r' < r$ with the region $r' > r$, $2(\alpha w - \ln \mathcal{D})$ with zero entanglement between left and right sides, through the constriction. Thus we conclude that

$$\ln \mathcal{D} = \ln g_{\mathrm{UV}} - \ln g_{\mathrm{IR}}. \tag{3.47}$$

Thus, the topological entropy of a gapped 2D system is equal to the change in impurity entropy of the corresponding 1D gapless edge theory under a change in CIBC corresponding to breaking the system into two pieces. This is a rather remarkable result since the topological entropy can be derived and analyzed in a system with no physical boundaries. A hand-waving explanation of this was given in [58]. Gapless edge modes must arise in a topological insulator in order to cancel a chiral anomaly [59–62]. When a region B is integrated out, we should also integrate over modes associated with the fictitious boundary of the region in order to integrate out an anomaly-free region. This effectively induces gapless edge modes in region A, to cancel those integrated out in region B. We note in passing that more generally, the local interactions associated with the constriction could lead to non-trivial boundary conditions not simply corresponding to perfect transmission or reflection. This would correspond to a different value of g_{IR} and probe other features of the topological insulator.

4. Bulk impurity effects

Another novel type of impurity entanglement entropy was studied in [20] and [22]. We consider the same type of model as discussed in subsection 3.3, a Luttinger liquid with a back-scatterer, considering the 1D formulation of the model. We now let the total system size $2R$ be finite with the back-scatterer in the center. Rather than considering the entanglement of a central region containing the origin with the rest, these authors considered instead the entanglement entropy of the region to the left of the constriction with the region to the right. With no back-scattering this is

$$S = \frac{c}{6}\ln\left(\frac{R}{a}\right). \tag{4.1}$$

With relevant backscattering, the 1D wire is effectively broken into two disconnected parts at long length scales so we might expect the entanglement entropy to vanish asymptotically.

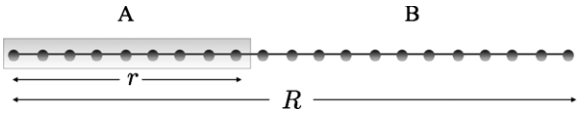

Figure 10. Schematic picture of a chain of total length R with OBC. The system has been cut into two parts A and B. Sub-system A, of length r, includes one open end.

This was studied numerically using DMRG in a critical Heisenberg XXZ spin chain with Hamiltonian

$$H = \sum_j J_j \left[\left(S_j^x S_{j+1}^x + S_j^y S_{j+1}^y \right) + \Delta S_j^z S_{j+1}^z \right]. \tag{4.2}$$

For uniform couplings, this model is in a gapless Luttinger liquid phase for $-1 < \Delta \leqslant 1$. Here $J_j = 1$ for all links except for one in the middle of the chain where it has the value J_{imp} with $0 < J_{\text{imp}} < 1$. This weakened link is a relevant perturbation for $\Delta > 0$ but irrelevant for $\Delta < 0$. The DMRG results were consistent with $S/\ln R$ going to zero at large R for $0 < \Delta \leqslant 1$ but going to $(1/6)$, the expected $c = 1$ value, for $-1 < \Delta < 0$. A quantitative theory of the R-dependence has not yet been developed, as far as we know.

The entanglement of a finite section of an infinite chain of free electrons with interface defects at the boundary of the finite section has been considered [21] and the position of the defect has been varied [67]. Properties of the impurity entanglement in the $s = 1/2$ XX chain in a transverse field where the field strength is perturbed at a single central site have also been investigated [68, 69] and entanglement in the quantum Ising chain with a time-dependent interface defect has been studied [70]. It is also possible to define models with conformal interfaces [71] where analytical results for the entanglement becomes possible. Entanglement in spatially inhomogeneous systems have also been considered [72].

5. Alternating and oscillating parts of the entanglement entropy

5.1. Open boundary induced alternation

As discussed in [23, 73], in the case of AF spin chains with OBC, the von Neumann entropy can be written as a sum of two contributions:

$$S(r, R) = S_{\text{U}}(r, R) + (-1)^r S_{\text{A}}(r, R). \tag{5.1}$$

The uniform part $S_{\text{U}}(r, R)$, in the case where the block of size r contains one open end (depicted in figure 10), is given by the CFT result [12], equation (3.17):

$$S_{\text{U}}(r, R) = \frac{c}{6} \ln \left[\frac{2R}{a\pi} \sin \left(\frac{\pi r}{R} \right) \right] + \ln g + s_1/2, \tag{5.2}$$

where $\ln g$ is the boundary entropy introduced in [11] and s_1 is a non-universal constant. $S(r, R)$ can be exactly computed numerically using either DMRG or exact diagonalization (ED). For the $S = 1/2$ XXZ chain,

$$\mathcal{H}_{\text{xxz}} = J \sum_{r=1}^{R-1} \left(S_r^x S_{r+1}^x + S_r^y S_{r+1}^y + \Delta S_r^z S_{r+1}^z \right), \tag{5.3}$$

which is critical for $|\Delta| \leqslant 1$, there is a special point at $\Delta = 0$ (XX point) where the spin chain is equivalent to free fermions. There, one can numerically compute the von Neumann entropy

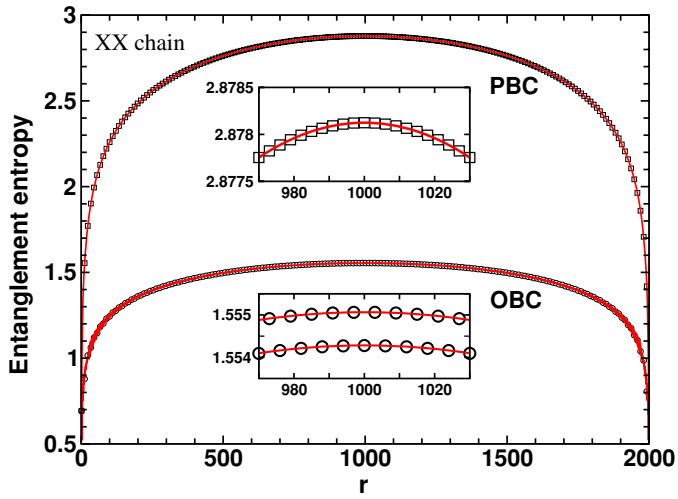

Figure 11. Results from ED of XX chains with $R = 2000$ spins $1/2$. The von Neumann entropy $S(r, R = 2000)$ is plotted versus the subsystem size r for PBC (upper symbols) and OBC (lower symbols); the insets shows zooms around the chain center. The full lines are fits: equation (5.4) with $s_1 = 0.726$ for PBC. In the OBC case, uniform and staggered terms $\frac{0.055-(-1)^r 0.25}{\frac{R}{\pi}\sin(\frac{\pi r}{R})}$ have been added to equation (5.2). Reprinted with permission from Laflorencie N *et al* 2006 *Phys. Rev. Lett.* **96** 100603. Copyright (2006) by the American Physical Society.

[74, 75] over for very large systems using ED, as shown in figure 11 both for PBC and OBC with $R = 2000$ sites. See also the review by Peschel and Eisler in this issue [76]. For periodic chains, the numerical results for the entropy are very well described by the expression [12], equation (3.18):

$$S(r, R) = \frac{c}{3} \ln \left[\frac{R}{a\pi} \sin \left(\frac{\pi r}{R} \right) \right] + s_1, \tag{5.4}$$

with $c = 1$ and $s_1 \simeq 0.726$ as predicted in [77] for free fermions. On the other hand for OBC, besides the uniform logarithmic increase equation (5.2), there are additional uniform and staggered terms which decay away from the boundary $(0.055 - (-1)^r 0.25) \big/ \left[\frac{R}{\pi} \sin \left(\frac{\pi r}{R} \right) \right]$. Not predicted by CFT, the origin of the alternating term has been carefully investigated using ED and DMRG for critical XXZ chains in [23]. Such a phenomenon has also been observed in several other cases where DMRG were applied for open systems. As discussed above, in [22] Peschel and co-workers, studying the effect of interface defects in critical spin chains, reported the observation of such oscillations. Fermions or bosons confined in 1D geometries with OBC are also affected by such a modulation, as reported for fermionic [78–80] and bosonic [81] Hubbard-like models. An interesting example of critical spin chain is the $S = 1$ bilinear–biquadratic model

$$\mathcal{H} = \sum_{r=1}^{R-1} [\cos\theta(\vec{S}_r \cdot \vec{S}_{r+1}) + \sin\theta(\vec{S}_r \cdot \vec{S}_{r+1})^2], \tag{5.5}$$

which displays conformally invariant critical points at $\theta = \pi/4$ with $c = 2$ and at $\theta = -\pi/4$ with $c = 3/2$. As studied by Legeza and co-workers [78], the dominant correlations at $k = \pi$ for $\theta = -\pi/4$ and $k = 2\pi/3$ for $\theta = \pi/4$ show up in the von Neumann entropy as displayed in figure 12. However, a quantitative study of this boundary-induced term was not achieved in [78] where the authors simply performed a fit to the expression equation (5.2) restricting

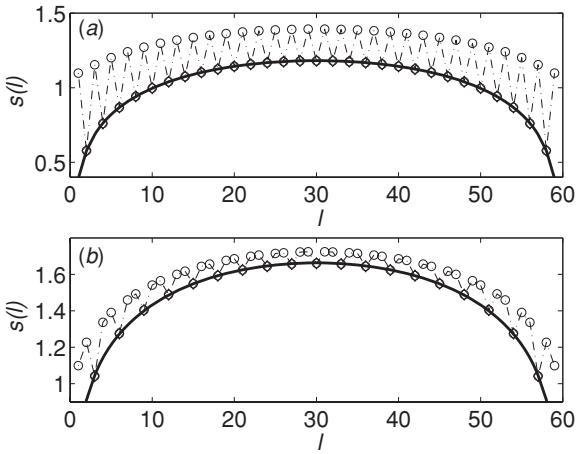

Figure 12. von Neumann entropy computed by DMRG for the $S = 1$ bilinear–biquadratic model equation (5.5) on open chains for two critical points: (*a*) $\theta = -\pi/4$ and (*b*) $\theta = \pi/4$. Black lines are fits to expression (5.2) with (*a*) $c = 1.5$ and (*b*) $c = 2$. Reprinted with permission from Legeza Ö *et al* 2007 *Phys. Rev. Lett.* **99** 087203. Copyright (2007) by the American Physical Society.

to the lower points: $r = 2p$ ($\theta = -\pi/4$) and $r = 3p$ ($\theta = \pi/4$), with p integer. Another interesting case has been studied with DMRG by Roux and collaborators [80] in the context of spin-3/2 fermionic cold atom with attractive interactions confined in a 1D optical lattice. They also found OBC-induced non-uniform features in the von Neumann entropy $S(r, R)$ with $2k_F$ oscillations that also appear in the local density and kinetic energy $t(r, R)$. Oscillations of $S(r, R)$ and $t(r, R)$ appear to be directly related as displayed in figure 13. Varying the parameters of the fermionic Hubbard model studied in this context [80], there is a critical point with $c = 3/2$ which separates two phases with $c = 1$. Imposing the non-uniform part of the von Neumann entropy to be directly proportional to the non-uniform part of the kinetic energy, a good fit was obtained by Roux and collaborators with a clear jump in the central charge $c = 1 \to 3/2$ at the critical point [80].

5.2. *Valence bond physics*

Open boundary-induced oscillations in the entanglement entropy appear to be a quite general phenomenon, as also observed in a valence bond physics framework [55, 56, 82, 83]. For $SU(2)$ invariant spin systems, the $S_{\text{tot}} = 0$ sector can be studied by quantum Monte Carlo simulations in the valence bond basis [84]. In such a framework, one can define a valence bond entropy which displays surprising similarities with the von Neumann entropy [55, 56, 82, 83]. For random bond spin chains, Refael and Moore [54] achieved a very nice calculation of the von Neumann entropy, simply observing that for a single valence bond configuration (as depicted for instance in figure 14(*a*)), the entropy is just given by $N(r) \times \ln 2$, where $N(r)$ is the number of singlet bonds crossing the interface between the two sub-systems. Such an idea was successfully checked numerically in the random bond case [55, 85, 86]. In the disorder-free case, while the ground-state is a highly non-trivial superposition of a huge number of valence bond configurations, such a phenomenological approach appeared to be extremely useful to understand the oscillating features [23]. Indeed, since the translational invariance is explicitly broken by the open ends, there is tendency toward dimerization near the open edges.

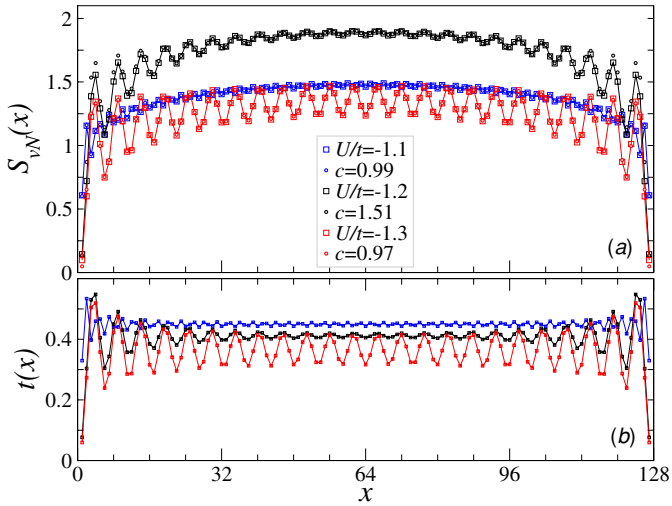

Figure 13. von Neumann block entropy $S(x)$ for a block of size x (a) and local kinetic energy $t(x)$ (b) around the critical point of a spin-3/2 fermionic Hubbard model with attractive interactions $U/t = -1.1, -1.2, -1.3$ for fixed $V/t = -2$ and $n = 0.75$ with $L = 128$. Fits using the oscillations of the local kinetic energy term (b) are quite accurate, allowing for the determination of the central charge c. Reprinted with permission from Roux G *et al* 2009 *Eur. Phys. J.* B **68** 293. Copyright (2009) by Springer Science & Business Media.

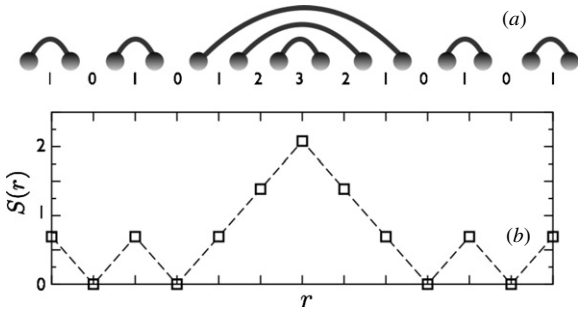

Figure 14. (a) Schematic picture for a particular valence bond state favored by OBC. The number of crossing bonds $N(r)$ is given. (b) Corresponding von Neuman entropy.

Such an effect can be computed very precisely (see below) but already at a qualitative level, this short-range singlet formation in the vicinity of open boundaries can be interpreted as an alternation of *strong* and *weak* bonds along the chain, thus leading to a similar alternation of $S(r, R)$. Indeed, the boundary spin at $r = 1$ will have a strong tendency to form a singlet pair with its only partner on the right-hand side. On the other hand the spin located at $r = 2$ will be consequently less entangled with its right partner at $r = 3$ since it already shares a strong entanglement with its left partner. A typical valence bond configuration favored by OBC is depicted in figure 14(a) with the corresponding entropy (b). Such a qualitative interpretation in term of 'weak-strong' modulation is directly related to OBC-induced Friedel-like oscillations that one can investigate in a more quantitative way, as we do now.

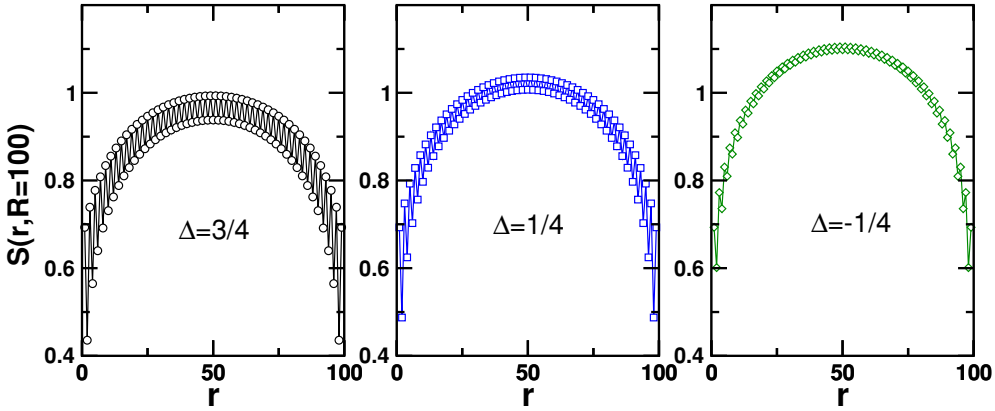

Figure 15. von Neuman entropy of XXZ chains of lengths $R = 100$ with OBC computed with DMRG for various anisotropies Δ.

5.3. Entropy oscillation and dimerization for critical XXZ chains

The alternating part $S_A(r, R)$ has been studied in [23] all along the critical regime of the XXZ chain $|\Delta| \leqslant 1$. DMRG results for $S(r, R) = S_U(r, R) + (-1)^r S_A(r, R)$ are shown in figure 15 for $R = 100$ and various Δ. One sees immediately that the oscillating part varies with Δ and decays faster in the ferromagnetic regime. More quantitatively, it was shown [23] that the alternating part $S_A(r, R)$ is directly proportional to the alternating term in the energy density. The energy density for XXZ spin chains

$$\langle h_r \rangle = \left\langle S_r^x S_{r+1}^x + S_r^y S_{r+1}^y + \Delta S_r^z S_{r+1}^z \right\rangle \tag{5.6}$$

is uniform in periodic chains. On the other hand, an open end breaks translational invariance and there will be a slowly decaying alternating term or 'dimerization' in the energy density

$$\langle h_r \rangle = E_U(r) + (-1)^r E_A(r), \tag{5.7}$$

where $E_A(r)$ becomes nonzero near the boundary and decays slowly away from it. $E_A(r)$ is obtained by Abelian bosonization modified by OBC [87]. In the critical region $|\Delta| \leqslant 1$, one gets [8, 23]

$$E_A(r, R) \propto \frac{1}{\left[\frac{2R}{\pi} \sin\left(\frac{\pi r}{R}\right)\right]^K}, \tag{5.8}$$

where K is the Luttinger liquid parameter defined as $K = \pi/(2(\pi - \cos^{-1}\Delta))$ so that $K = 1$ for an XX spin chain, $K = 1/2$ for the AF Heisenberg model and $K \to \infty$ for the ferromagnetic Heisenberg case. Based on DMRG data obtained [23] on critical open chains of sizes $200 \leqslant R \leqslant 1000$, we find a proportionality between S_A and E_A. More precisely, plotting S_A as a function of $-E_A$ for various values of the anisotropy Δ in figure 16, we find a linear relation $S_A = -\alpha E_A$ with a prefactor perfectly described by $\alpha = \mu/\sin\mu$, as shown in the inset of figure 16, with $\mu = \cos^{-1}\Delta$. We note that the velocity of excitations for the XXZ model is given by $v = \pi(\sin\mu)/(2\mu)$ so that we may write this relation as

$$S_A = -(\pi a^2/2v) E_A, \tag{5.9}$$

where we have introduced the lattice spacing, a, to make the entanglement entropy a dimensionless quantity (E_A has dimensions of energy per unit length). We emphasize that

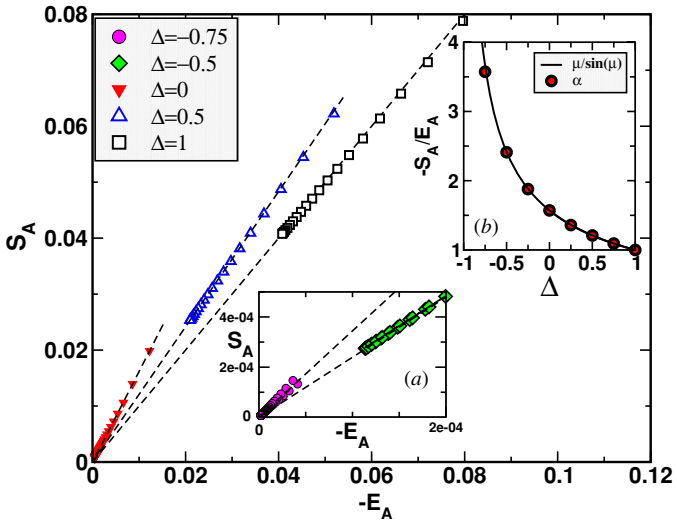

Figure 16. Linear behavior of the alternating part of the entanglement entropy, S_A, as a function of the alternating energy density, $-E_A$, both computed using DMRG on critical open XXZ chains of size $200 \leqslant R \leqslant 1000$ for a few values of the anisotropy Δ. Data from ED at $\Delta = 0$ are also shown for $R = 2000$. Dashed lines are linear fits of the form $S_A = -\alpha E_A$ (see the text). The inset (*a*) is a zoom close to 0, showing data for $\Delta = -3/4$ and $-1/2$. The inset (*b*) shows the prefactor α versus Δ extracted from the numerical data (circles), for a larger set of values of Δ, which is compared with $\pi/2v = \mu/\sin\mu$, $\mu = \cos^{-1}\Delta$. Reprinted with permission from Laflorencie N *et al* 2006 *Phys. Rev. Lett.* **96** 100603. Copyright (2006) by the American Physical Society.

equation (5.9) even holds for the Heisenberg model (with a proportionality coefficient $\alpha = 1$) where both E_A and S_A display the same logarithmic corrections. Indeed, at the Heisenberg point, $\Delta = 1$, equation (5.8) will have some logarithmic corrections due to the presence of a marginally irrelevant coupling constant in the low energy Hamiltonian, leading to [8, 23] $E_A(r) \propto 1/[\sqrt{r}(\ln r)^{3/4}]$ in the limit $R \to \infty$. It is highly non-trivial to include both the log corrections and the finite size effects in $E_A(r, R)$. However, there is a simple result at $r = R/2$. Including the cubic term in the β-function for the marginal coupling constant, and other higher order corrections [88], this becomes:

$$E_A\left(\frac{R}{2}, R\right) = a_0 \frac{1 + a_2/[\ln(R/a_1)]^2}{\sqrt{R}[\ln(R/a_1) + (1/2)\ln\ln(R/a_1)]^{\frac{3}{4}}}, \tag{5.10}$$

where a_0, a_1 and a_2 are constants. If one allows a frustrating second neighbor coupling J_2 in the chain, at $J_2^c = 0.241\,167J$, this model is at the critical point between gapless and gapped spontaneously dimerized phase and the marginal coupling constant, and hence the log corrections are expected to vanish here. In both cases ($J_2 = 0$ and $J_2 = J_2^c$), we found proportionality between S_A and E_A, as shown in figure 17. The sum $E_A(R/2, R) + \alpha S_A(R/2, R)$ is found to rapidly decay as a power law, with a power ~ 2.5 (see figure 17). Interestingly, for $J_2 = 0.241\,167$, again linearity is observed, but with a prefactor $\alpha \simeq 1.001\,689$ not related to the spin velocity, v, which we have determined to be $v \simeq 1.174(1)$ [53]. Hence, equation (5.9) does not hold in this case.

We emphasize that this alternating term in $S(r, R)$ is universal and should *not* be regarded as a correction due to irrelevant operators. First of all, it is not a 'correction', since it is alternating. Secondly, it decays with the same power law as $E_A(r, R)$ which is seen to be a property of the fixed point, not the irrelevant operators. (However, for the Heisenberg model,

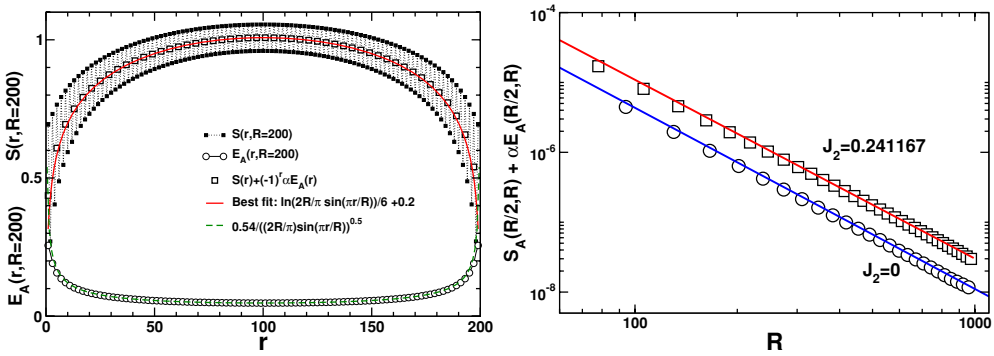

Figure 17. (*a*) Entanglement entropy $S(r)$ (black squares) and alternating part of the energy density $E_A(r)$ (open circles) computed with DMRG at J_2^c for $R = 200$ sites. The dashed line is equation (5.8). The uniform part of $S(r)$, obtained by taking $S(r) + (-1)^r \alpha E_A(r)$ with $\alpha = 1.001\,699$, is represented by open squares. The best fit, shown by a red curve, is indicated on the plot. (*b*) Comparison between the alternating part S_A and E_A (equation (5.9)) from DMRG with $m = 512$ states, for Heisenberg models. Power-law decay of $S_A(R/2, R) + \alpha E_A(R/2, R)$ drawn in a log–log plot, with $\alpha = 1$ for the nearest-neighbor chain ($J_2 = 0$) and $\alpha = 1.001\,69$ at the critical second neighbor coupling $J_2 = 0.241\,167$. Lines are power-law fits: $\sim R^{-2.56}$ for $J_2 = 0.241\,167$ and $R^{-2.59}$ for $J_2 = 0$. (*a*) and (*b*) are respectively reprinted from [8]. Copyright (2007) by IOP Publishing Ltd, and with permission from Laflorencie N *et al* 2006 *Phys. Rev. Lett.* **96** 100603. Copyright by the American Physical Society.

$\Delta = 1$, the log factor in $E_A(r, R)$ *is* due to the marginally irrelevant operator.) The presence of a universal alternating term in $S(r, R)$ is connected with the antiferromagnetic nature of the Hamiltonian (not appearing, for example, in the quantum Ising chain [16]) and *does not* seem to follow from the general CFT treatment in [12]. An analytic derivation of this phenomena remains an open problem.

5.4. Spin-chain Kondo model

We now turn to the spin-chain Kondo model equation (3.32). In previous sections, only the uniform part of the impurity part of the von Neumann entropy has been investigated. Here we focus on the alternating part which is also present for impurity problems. We want to isolate the impurity contribution in the alternating part of $S(r, R)$. Following our fundamental definition of $S_{\rm imp}$, equation (3.34), it is also possible to define the alternating part of the impurity entanglement entropy:

$$S^A_{\rm imp}(J'_K, r, R) \equiv S_A(J'_K, r, R) - S_A(1, r-1, R-1). \tag{5.11}$$

As before, we have subtracted S_A when the impurity is absent, in which case both r and R are reduced by 1 and the coupling at the end of this reduced chain, linking site 2 to 3 and 4, has unit strength. Applying this definition to numerical data involves some subtleties. First of all S_A is only defined up to an overall sign. Secondly, when calculating $S_A(1, r-1, R-1)$, we define this as $-S_A(1, r', R')$ with $R' = R-1$ since the shift from r to $r-1$ implies a sign change in the alternating part. For convenience, we have therefore always exploited this degree of freedom to use a sign convention that makes the resulting $S^A_{\rm imp}$ positive in all cases. In figure 18, we show data for the total entanglement entropy along with the extracted alternating parts and the resulting $S^A_{\rm imp}$ for both $R = 102$ even and $R = 101$ odd. As was the case for the uniform part of $S_{\rm imp}$ (figure 6), we do not observe any special features in $S^A_{\rm imp}(r)$ for fixed R, J'_K associated

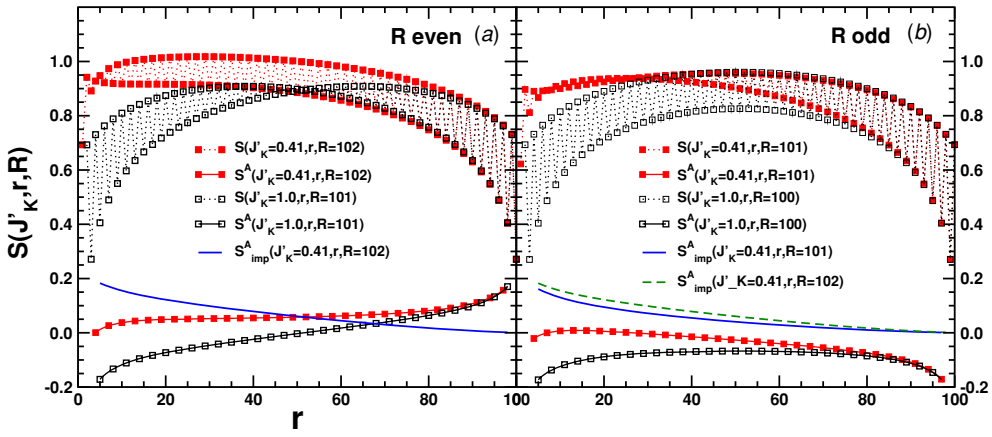

Figure 18. (*a*) DMRG results for the total entanglement entropy, $S(J'_K, r, R)$ for a 102 site spin chain at J_2^c, with a $J'_K = 0.41$ Kondo impurity (■) along with $S(J'_K = 1, r-1, R-1)$ (□). For both cases is the extracted alternating part shown along with the resulting $S^A_{\rm imp}(J'_K = 0.41, r, R = 102)$ for R even. (*b*) DMRG results for the total entanglement entropy, $S(J'_K, r, R)$ for a 101 site spin chain at J_2^c, with a $J'_K = 0.41$ Kondo impurity (■) along with $S(J'_K = 1, r-1, R-1)$ (□). For both cases is the extracted alternating part shown along with the resulting $S^A_{\rm imp}(J'_K = 0.41, r, R = 101)$ for R odd. For comparison, we also show $S^A_{\rm imp}(J'_K = 0.41, r, R = 102)$ for R even from panel (*a*) (dashed line). Reprinted from [8]. Copyright (2007) by IOP Publishing Ltd.

with the length scale ξ_K and in all cases $S^A_{\rm imp}$ decays monotonically with r. On the other hand, a possible scaling form for $S^A_{\rm imp}$ was suggested in [8]. For $J'_K = 1$, we have seen above that the alternating part of the entanglement entropy, $S_{\rm A}$, is proportional to the alternating part in the energy, $E_{\rm A}$, which for $J_2 = J_2^c$ can be written as follows: $E_{\rm A}(r) = f(r/R)/\sqrt{r}$ for some scaling function f. A generalization of the above formula to the case $J'_K \neq 1$ implies that $S^A_{\rm imp}\sqrt{r}$ should be a scaling function, $f(r/R, r/\xi_K)$. DMRG results for $S^A_{\rm imp}\sqrt{r}$ for fixed r/R are shown in figure 19 for a range of J'_K and R. The values for ξ_K used to attempt the scaling are the ones previously used for the scaling of the uniform part (figure 6). Clearly the results for $S^A_{\rm imp}\sqrt{r}$ follow the expected scaling form.

6. Impurity entanglement in gapped spin chains

In previous sections, the focus has largely been on work considering critical systems. The general case of entanglement in massive field theories will be reviewed elsewhere in this issue [89]. However, impurity entanglement in systems with a gap, corresponding to massive field theories with a finite correlation length ξ, has also been considered. In this case, the generalization of equation (1.2) to one-dimensional systems with a gap becomes [12]

$$S(r) \sim \frac{c}{6} \ln\left(\frac{\xi}{a}\right). \tag{6.1}$$

So far, mainly two models have been studied, $s = 1$ chains [90, 91] at the AKLT point [92, 93] and $s = 1/2$ $J_1 - J_2$ chains [8] at the Majumdar–Ghosh point, $J_2 = J_1/2$ [94]. While the $s = 1$ spin chain at the AKLT point has a correlation length $\xi = 1/\ln(3)$, the spin correlations in the $s = 1/2$ chain at the MG point do not extend beyond the nearest neighbor and the correlation length is effectively zero.

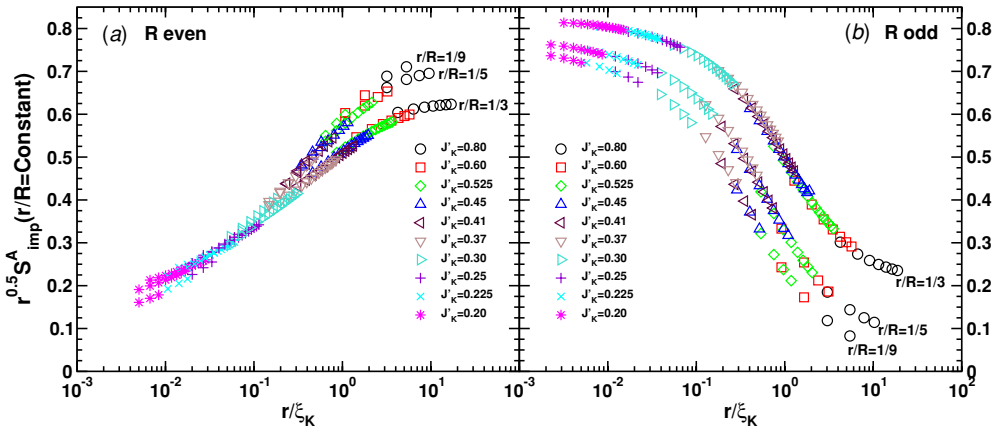

Figure 19. $\sqrt{r}S^A_{\rm imp}$ for fixed r/R and a range of couplings J'_K at J_2^c. (*a*) For R even and (*b*) for R odd. The values of ξ_K used are obtained from the scaling of $S_{\rm imp}$ achieved in figure 6. DMRG results with $m = 256$ states. Reprinted from [8]. Copyright (2007) by IOP Publishing Ltd.

6.1. The $s = 1$ ALKT chain

Boundary effects in the entanglement entropy of a $s = 1$ chain were studied in [91] building on earlier work [90]. The model considered was a special case of equation (5.5), the antiferromagnetic $s = 1$ Heisenberg chain including a $1/3$ bi-quadratic term:

$$H = \sum_{j=-N_l+1}^{L+N_r-1} \left[\vec{S}_j \cdot \vec{S}_{j+1} + \frac{1}{3}(\vec{S}_j \cdot \vec{S}_{j+1})^2 \right]. \; s = 1. \tag{6.2}$$

For this special value of the bi-quadratic coupling, termed the AKLT point, the ground state is known exactly [92, 93] and this fact was exploited to perform exact calculations of the entanglement entropy. The entanglement of a sub-systems consisting of the *central* section of the chain, $1 \ldots L$, with the remaining *left and right* parts of the chain was considered. Here N_l and N_r describe the size of the left and right parts of the system and it was shown [91] that the boundary effects in the entanglement entropy decay exponentially fast with N_l, N_r on a length scale equal to the correlation length $\xi = 1/\ln(3)$. Hence, impurity effects in the entanglement impurity are in this case rather minor. In contrast, by considering a subsystem including the boundary (the impurity), the impurity entanglement in the Majumdar Ghosh model can be rather pronounced.

The partial concurrence of the two effective $s = 1/2$ spins at the end of an open $s = 1$ chain has also been studied [31].

6.2. The Majumdar–Ghosh model

At the special point $J_2 = J_1/2$, often referred to as the Majumdar–Ghosh [94, 95, 96] (MG) point, the spin-chain model equation (3.32) with $J'_K = 1$ is exactly solvable. The spin chain has a gap and for R *even*, in the presence of periodic boundary conditions, a twofold degenerate ground state of nearest-neighbor dimers either between sites $2n + 1$ and $2n + 2$ or $2n + 2$ and $2n + 3$, $n \geqslant 0$, with energy $E = -3RJ/8$. With open boundary conditions, for R *even*, the ground state is non-degenerate with dimers between sites $2n + 1$ and $2n + 2$, $n = 0, \ldots, (R - 1)/2$, and with the same energy as the periodic case, $E = -3RJ/8$.

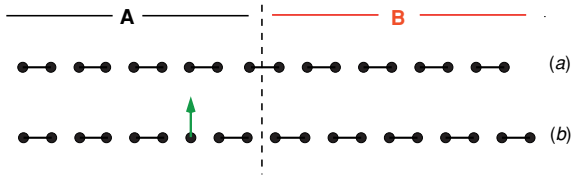

Figure 20. MG state divided in two regions A and B. (a) The total number of site R is even and the ground state is a singlet. (b) When R is odd, the ground state contains a soliton $\uparrow$. Reprinted from [8]. Copyright (2007) by IOP Publishing Ltd.

See figure 20(a). If one now instead considers R *odd*, an exact form for the ground state wavefunction and energy is not known but a very precise variational form can be developed [8, 97–102]. For R odd, it is natural to consider states of the following form:

$$|n\rangle \equiv |\overbrace{- \ldots -}^{n} \uparrow - \ldots -\rangle. \tag{6.3}$$

Here, $-$ indicates a singlet between site r and $r+1$ and $n = 0, \ldots, N_d - 1 = (R-1)/2$ refers to the number of dimers to the left of the soliton, with N_d the total number of dimers. See figure 20(b). Such states are often called *thin soliton* states (TS-states) because the soliton resides on a single site and is not 'spread' out over several sites as would have been the case if one had included states with valence bonds longer than between nearest-neighbor sites. Note that the soliton only resides on the odd sites of the lattice, $r = 1, 3, \ldots, R$. It is important to realize that the TS-state as defined are not orthornormal and even though it is straightforward to form linear combinations $|m\rangle$ that are orthogonal [101, 102] through the transformation $|m=0\rangle \equiv |n=0\rangle$, $|m\rangle \equiv (2/\sqrt{3})\,[|n\rangle + (1/2)|n-1\rangle]$ $m \geqslant 1$, one finds that for the purpose of calculating the entanglement this orthogonalization is less useful at the initial stage of calculating the entanglement entropy.

If only the $\Uparrow$ state of the ground state doublet for R odd is considered, one can write a thin soliton ansatz (TS-ansatz) for the ground state wavefunction:

$$|\Psi_{\mathrm{TS}}^{\Uparrow}\rangle \simeq \sum_{n=0}^{N_d} \psi_n^{\mathrm{sol}} |n\rangle. \tag{6.4}$$

It can be shown that the restriction to the $\Uparrow$ state is not important since any linear combination of the degenerate $\Uparrow$ and $\Downarrow$ states will yield the same entanglement entropy [8]. The components of the ground state wavefunction, ψ_n^{sol}, can be obtained in a variational manner or through a simple analytical estimate [8]

$$\psi_n^{\mathrm{sol}} \simeq \sqrt{\frac{2}{N_d+2}} \sin\left(\frac{\pi(2n+2)}{R+3}\right). \tag{6.5}$$

With the ψ_n^{sol} determined we can proceed with the calculation of the entanglement entropy. Due to the dimerization of the ground state, one sees that for R even (and open boundary conditions) $S(r, R)$ simply oscillates with r between $\ln(2)$ and 0 depending on whether r is a site at the beginning or end of a dimer, respectively. With a $J_K' \neq 1$ in equation (3.32), the entanglement is much richer and exact results are not available; however, *very precise* variational calculations [8] of $S(r, R)$ are possible. Let us first consider R odd and $J_K' = 1$ with r *odd*. We first divide the system into two parts (A, B) at r and let $|\phi\rangle$ denote a basis for $1 \ldots r$ and $|\psi\rangle$ a basis for $r+1 \ldots R$. If the soliton is to the left of r and since r is odd the

division between A and B will not 'cut' a dimer. However, if the soliton is to the right of r the division will cut a dimer and we effectively get an additional soliton at the end of the A space leading to the following three separate cases for $|\psi_i\rangle$ and $|\phi_j\rangle$ distinguished by the position of the soliton:

$$|\psi_1\rangle = \sum_{n=0}^{\frac{r-1}{2}} \psi_n^{\mathrm{sol}} |\overbrace{- \ldots -}^{n} \uparrow - \ldots -\rangle, |\phi_1\rangle = |\overbrace{- \ldots -}^{\frac{R-r}{2}}\rangle$$

$$|\psi_2\rangle = |\overbrace{- \ldots -}^{\frac{r-1}{2}} \uparrow\rangle, |\phi_2\rangle = \sum_{n=0}^{\frac{R-r}{2}-1} \psi_{\frac{r+1}{2}+n}^{\mathrm{sol}} |\downarrow \overbrace{- \ldots -}^{n} \uparrow - \ldots -\rangle$$

$$|\psi_3\rangle = |\overbrace{- \ldots -}^{\frac{r-1}{2}} \downarrow\rangle, |\phi_3\rangle = \sum_{n=0}^{\frac{R-r}{2}-1} \psi_{\frac{r+1}{2}+n}^{\mathrm{sol}} |\uparrow \overbrace{- \ldots -}^{n} \uparrow - \ldots -\rangle. \quad (6.6)$$

With these definitions it immediately follows that

$$|\Psi_{\mathrm{TS}}^{\Uparrow}\rangle = |\psi_1\rangle|\phi_1\rangle + \frac{1}{\sqrt{2}}\left[|\psi_2\rangle|\phi_2\rangle - |\psi_3\rangle|\phi_3\rangle\right]. \quad (6.7)$$

Again we emphasize that the above form follows since the system was divided into two parts at r and since r *is odd*. The states $|\phi_i\rangle$ and $|\psi_j\rangle$ are clearly not orthonormal; however, by explicitly orthonormalizing the states $|\psi_j\rangle$ region B can be traced out and the reduced density matrix ρ for region A determined. It is straightforward to generalize this approach to the case where r is even (and R is odd with $J_K' = 1$). Results from such a calculation is shown in figure 21(*a*) where they are compared with DMRG results. Excellent agreement is observed. For comparison, results for $S_{\mathrm{u}}(J_K' = 1, r, R = 201)$ and $S_{\mathrm{U}}(J_K' = 1, r, R = 200)$ are also shown in figure 21(*a*). The difference of these two uniform parts yields S_{imp}. The influence of the impurity spin coupled with $J_K' = 1$ is clearly visible and extends over the *entire* range of r.

As already outlined in section 3.2, the entanglement of the impurity spin with the bulk of the chain is sizable (one might even say maximal) even when $J_K' = 0$. With some additional algebra, it is possible to extend the thin-soliton approach also to this case [8] by considering a decoupled impurity entangled with a bulk chain of *odd* length $R - 1$. Hence, the TS-ansatz can be applied to the bulk chain and precise variational results are obtained. It is crucial to note that the impurity spin and the bulk chain form a singlet state even though their coupling, J_K', is zero. That is, we consider the $J_K' \to 0$ limit of the entanglement entropy. Results obtained from the TS-ansatz are shown in figure 21(*b*) where they are compared to DMRG results obtained using spin inversion. The DMRG calculations are performed on systems where the impurity spin is explicitly included resulting in a fourfold degenerate ground state consisting of a singlet and a triplet. The application of spin-inversion symmetry is therefore necessary in order to distinguish the singlet state of interest from the degenerate triplet state. The agreement between the numerical and variational results in figure 21(*b*) is excellent; the small discrepancies visible at a few values of r are due to complications using spin inversion [103] in the DMRG calculations specific to this value of J_2. For comparison, results for $S_{\mathrm{u}}(J_K' = 0, r, R = 200)$ and $S_{\mathrm{U}}(J_K' = 1, r, R = 199)$ are also shown in figure 21(*b*). The difference of these two uniform parts yields S_{imp} which is non-zero throughout the system.

Perhaps surprisingly, it is possible to obtain a much more intuitive picture and yet still very precise by simply assuming that the states $|\phi_i\rangle$ and $|\psi_j\rangle$ are orthogonal. With this assumption

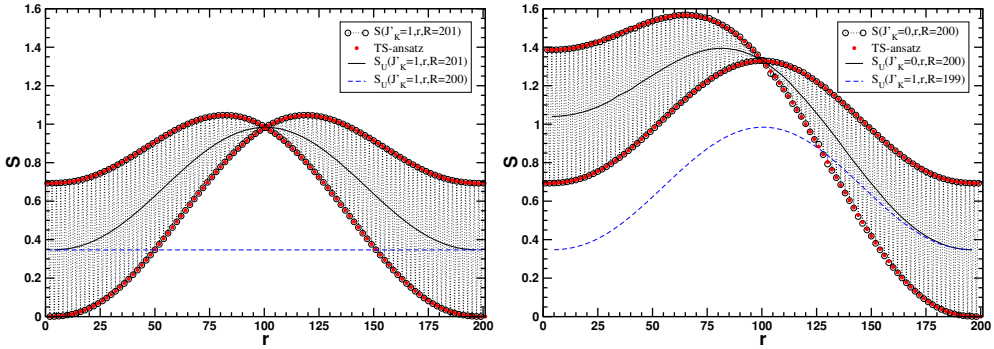

Figure 21. (*a*) DMRG results with $m = 256$ for $S(J'_K = 1, r, R = 201)$ for the spin-chain model with $J_2 = 1/2$ (MG model). The small solid circles represent the theoretical result obtained using the TS-ansatz. Also shown are the uniform parts $S_U(J'_K = 1, r, R = 201)$ and $S_U(J'_K = 1, r, R = 200)$, the difference of which is $S_{\rm imp}(J'_K = 1)$. (*b*) DMRG results with $m = 256$ for $S(J'_K = 0, r, R = 200)$ for the spin-chain model with $J_2 = 1/2$ (MG model). The small solid circles represent the theoretical result obtained using the TS-ansatz. Also shown are the uniform parts $S_U(J'_K = 0, r, R = 200)$ and $S_U(J'_K = 1, r, R = 199)$, the difference of which is $S_{\rm imp}(J'_K = 0)$.

it is easy to see from equation (6.7) that the reduced density matrix for region A (with R odd) is simply

$$\rho = \begin{pmatrix} p & 0 & 0 \\ 0 & \frac{1-p}{2} & 0 \\ 0 & 0 & \frac{1-p}{2} \end{pmatrix}, \qquad r \text{ odd}, \qquad \rho = \begin{pmatrix} 1-p & 0 & 0 \\ 0 & \frac{p}{2} & 0 \\ 0 & 0 & \frac{p}{2} \end{pmatrix}, \qquad r \text{ even}. \tag{6.8}$$

Here $p = \sum_{n=0}^{(r-1)/2} |\psi_n^{\rm sol}|^2 \sim r/R - \sin(2\pi r/R)/(2\pi)$ is the probability of finding the soliton in region A. From these expressions for ρ the entanglement entropy can easily be evaluated. In order to calculate $S_{\rm imp}$ the uniform part of S for an even length chain with $J'_K = 1$ is needed, but, as mentioned previously, this is simply $\ln(2)/2$ and it follows that

$$S_{\rm imp}(J'_K = 1, r, R) = -p\ln(p) - (1-p)\ln(1-p) \equiv S_{\rm imp}^{\rm SPE}, \qquad R \text{ odd}. \tag{6.9}$$

In this case the impurity entanglement arises solely from the entanglement of a single particle (the soliton) that is present in the ground-state and one therefore refers to this contribution as the single particle entanglement, $S_{\rm imp}^{\rm SPE}$. See figure 22(*b*).

With more effort an analogous calculation can be carried through for the case of R even and $J'_K = 0$. One finds [8]

$$S_{\rm imp}(J'_K = 0, r, R) = (1-p)\ln(2) = S_{\rm imp}^{\rm IVB}, \qquad R \text{ even}. \tag{6.10}$$

We see that in this case there is no contribution from the single particle entanglement as one would expect since there are no solitons (single particles) present in the ground state. Instead, the impurity entanglement is given purely by the impurity valence bond (IVB) (see section 3.2) where in the present case one identifies the probability that the IVB does not cross the boundary between regions A and B with the probability of finding a soliton in region A. See figure 22(*a*).

Some surprising observations can be found by performing numerical calculations of $S_{\rm imp}$ away from the MG point where the above variational calculations are quasi-exact. One finds [8] (i) $S_{\rm imp}$ for both even and odd R is non-zero over the entire range of r and is not limited

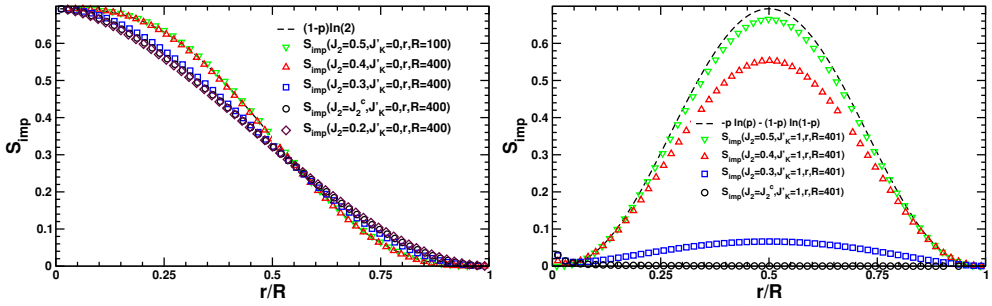

(*a*) (*b*)

Figure 22. (*a*) DMRG results with $m = 256$ for $S(J'_K = 0, r, R = 400)$ for the spin-chain model with $J_2/J = 0.2, J_2^c, 0.3, 0.4, 0.5$ shown along with the result for $S_{\rm imp}^{\rm IVB} = (1-p)\ln(2)$ with p calculated at $J_2/J = 0.5$ (dashed line). (*b*) DMRG results with $m = 256$ for $S(J'_K = 1, r, R = 401)$ for the spin-chain model with $J_2/J = J_2^c, 0.3, 0.4, 0.5$. The dashed line represents $S_{\rm imp}^{\rm SPE} = -p\ln(p) - (1-p)\ln(1-p)$ with p calculated at $J_2 = J/2$. Reprinted from [8]. Copyright (2007) by IOP Publishing Ltd.

by the correlation length which is effectively zero. (ii) $S_{\rm imp}(J'_K = 0, r, R)$ for R even changes only slightly when J_2 is decreased from $J_2 = J/2$ to $J_2 = J_c^2$ and for $J_2 \leqslant J_2^c$ in the gapless phase it appears not to change at all with J_2. In all cases, $0 \leqslant J_2 \leqslant J/2$, does the IVB picture seem to correctly describe $S_{\rm imp}$. This is illustrated in figure 22(*a*). IT is perhaps surprising that the IVB picture works relatively well for $J_2 < J_2^c$ where long-range valence bonds are present in the ground state. (iii) $S_{\rm imp}(J'_K = 1, r, R) \sim S_{\rm imp}^{\rm SPE}$ for R odd decreases rapidly with J_2 from $J/2$ to J_2^c where it vanishes. For $J_2 \leqslant J_2^c$, this part of the impurity entanglement is negligible. Hence, it seems likely that this fact is related to the system becoming gapless at J_2^c. This is illustrated in figure 22(*b*).

Finally we note that, the concurrence of the end spins in the dimerized $J_1 - J_2$ $s = 1/2$ model have been studied [31].

7. Conclusions

We have reviewed recent results related to the impurity contribution to the entanglement, $S_{\rm imp}$, arising from a quantum impurity or boundary. Most notably it has by now clearly been established that the entanglement can be dramatically changed by the presence of an impurity even in the case where the physical coupling to the impurity is zero. The role played by different boundary conditions in (1 + 1)-dimensional critical systems is well understood and in agreement with results from CFT. However, for the case of mixed boundary conditions (section 3.2), quantitative theory is not yet available and a detailed understanding of the R dependence of bulk impurity effects (section 4) would be desirable. A consistent picture of the entanglement of a qubit with the environment as described by the spin-boson problem and the entanglement arising from Kondo impurities has been developed based on established theory of Kondo systems. A more heuristic picture of impurity entanglement in gapped (and to a certain extent also critical) one-dimensional systems based on valence bond physics and matrix product states is emerging. Useful notions of single particle entanglement (SPE) and impurity valence bonds (IVB) have been introduced. Some details of this picture are still missing. As an example, how the single particle entanglement disappears as the system approaches criticality is still an open problem. Comparatively few results are available for

quantum impurity entanglement in two (and higher)-dimensional quantum systems and a detailed theory is still lacking.

Acknowledgments

We are grateful to F Alet, S Capponi, M-S Chang, J Cardy and M Mambrini for interesting discussions. This research was supported by NSERC (all authors), the CIFAR (IA) CFI (ESS). NL thanks LPT (Toulouse) for hospitality. Part of the numerical simulations have been performed on the WestGrid network. This work was made possible by the facilities of the Shared Hierarchical Academic Research Computing Network (SHARCNET:www.sharcnet.ca).

References

[1] von Neumann J 1927 *Gött. Nachr.* 273
[2] Wehrl A 1978 General properties of entropy *Rev. Mod. Phys.* **50** 221
[3] Cho S Y and McKenzie R H 2006 Quantum entanglement in the two-impurity Kondo model *Phys. Rev.* A **73** 012109
[4] Kopp A and Le Hur K 2007 Universal and measurable entanglement entropy in the spin-boson model *Phys. Rev. Lett.* **98** 220401
[5] Le Hur K, Doucet-Beaupre P and Hofstetter W 2007 Entanglement and criticality in quantum impurity systems *Phys. Rev. Lett.* **99** 126801
[6] Le Hur K 2007 Entanglement entropy, decoherence, and quantum phase transitions of a dissipative two-level system *Ann. Phys.* **323** 2208–40
[7] Mross D and Johannesson H 2009 The two-impurity Kondo model with spin–orbit interactions *Phys. Rev.* B **80** 155302
[8] Sørensen E S, Chang M-S, Laflorencie N and Affleck I 2007 Quantum impurity entanglement *J. Stat. Mech.* P08003
[9] Andrei N and Destri C 1984 Solution of the multichannel Kondo problem *Phys. Rev. Lett.* **52** 364
[10] Tsvelik A M and Wiegmann P B 1985 Exact solution of the multichannel Kondo problem, scaling, and integrability *J. Stat. Phys.* **38** 125
[11] Affleck I and Ludwig A W W 1991 Universal noninteger ground-state degeneracy in critical quantum systems *Phys. Rev. Lett.* **67** 161
[12] Calabrese P and Cardy J 2004 Entanglement entropy and quantum field theory *J. Stat. Mech.* P06002
[13] Cardy J and Peschel I 1988 Finite-size dependence of the free energy in two-dimensional critical systems *Nucl. Phys.* B **300** 377
[14] Holzhey C, Larsen F and Wilczek F 1994 Geometric and renormalized entropy in conformal field theory *Nucl. Phys.* B **424** 443
[15] Korepin V E 2004 Universality of entropy scaling in one-dimensional gapless models *Phys. Rev. Lett.* **92** 096402
[16] Zhou H-Q, Barthel T, Fjaerestad J and Schollwöck U 2006 Entanglement and boundary critical phenomena *Phys. Rev.* A **84** 050305
[17] Sørensen E S, Chang M-S, Laflorencie N and Affleck I 2007 Impurity entanglement entropy and the kondo screening cloud *J. Stat. Mech.* L01001
[18] Kitaev A and Preskill J 2006 Topological entanglement entropy *Phys. Rev. Lett.* **96** 110404
[19] Levin M and Wen X G 2006 Detecting topological order in a ground state wave function *Phys. Rev. Lett.* **96** 110405
[20] Levine G C 2004 Entanglement entropy in a boundary impurity model *Phys. Rev. Lett.* **93** 226402
[21] Peschel I 2005 Entanglement entropy with interface defects *J. Phys. A: Math. Gen.* **38** 4327
[22] Zhao J, Peschel I and Wang X Q 2006 Critical entanglement of xxz Heisenberg chains with defects *Phys. Rev.* B **73** 024417
[23] Laflorencie N, Sørensen E S, Chang M-S and Affleck I 2006 Boundary effects in the critical scaling of entanglement entropy in 1d systems *Phys. Rev. Lett.* **96** 100603
[24] Bose S 2003 Quantum communication through an unmodulated spin chain *Phys. Rev. Lett.* **91** 207901
[25] Christandl M, Datta N, Ekert A and Landahl A J 2004 Perfect state transfer in quantum spin networks *Phys. Rev. Lett.* **92** 187902

[26] Christandl M, Datta N, Dorlas T C, Ekert A, Kay A and Landahl A J 2005 Perfect transfer of arbitrary states in quantum spin networks *Phys. Rev.* A **71** 032312
[27] Burgarth D and Bose S 2005 Perfect quantum state transfer with randomly coupled quantum chains *N. J. Phys.* **7** 135
[28] Burgarth D, Giovannetti V and Bose S 2005 Efficient and perfect state transfer in quantum chains *J. Phys. A: Math. Gen.* **38** 6793
[29] Wójcik A, Luczak T, Kurzyński P, Grudka A, Gdala T and Bednarska M 2005 Unmodulated spin chains as universal quantum wires *Phys. Rev.* A **72** 034303
[30] Plenio M B and Semião F L 2005 High efficiency transfer of quantum information and multiparticle entanglement generation in translation-invariant quantum chains *N. J. Phys.* **7** 73
[31] Campos Venuti L, Degli Esposti Boschi C and Roncaglia M 2006 Long-distance entanglement in spin systems *Phys. Rev. Lett.* **96** 247206
[32] Campos Venuti L, Degli Esposti Boschi C and Roncaglia M 2007 Qubit teleportation and transfer across antiferromagnetic spin chains *Phys. Rev. Lett.* **99** 060401
[33] Sodano P, Bayat A and Bose S 2008 Kondo cloud mediated long range entanglement after local quench in a spin chain arXiv:0811.2677
[34] Bayat A, Sodano P and Bose S 2008 Probing the Kondo regime with entanglement measures arXiv:0904.3341
[35] Calabrese P and Cardy J L 2007 Entanglement and correlation functions following a local quench: a conformal field theory approach *J. Stat. Mech.* P10004
[36] Klich I and Levitov L 2009 Quantum noise as an entanglement meter *Phys. Rev. Lett.* **102** 100502
[37] Klich I and Levitov L 2009 Many-body entanglement: a new application of the full counting statistics *Adv. Theor. Phys.* **1134** 36–45
[38] Hsu B, Grosfeld E and Fradkin E 2009 Quantum noise and entanglement generated by a local quantum quench arXiv:0908.2622
[39] Calabrese P and Cardy J L 2009 Entanglement entropy and conformal field theory arXiv:0905.4013
[40] Costi T and McKenzie R H 2003 Entanglement between a qubit and the environment in the spin-boson model *Phys. Rev.* A **68** 034301
[41] Sørensen E S and Affleck I 1996 Scaling theory of the Kondo screening cloud *Phys. Rev.* B **53** 9153
[42] Barzykin V and Affleck I 1996 The Kondo screening cloud: what can we learn from perturbation theory *Phys. Rev. Lett.* **76** 4959
[43] Barzykin V and Affleck I 1998 Screening cloud in the k-channel Kondo model: perturbative and large-k results *Phys. Rev.* B **57** 432
[44] Anderson P W, Yuval G and Hamann D R 1970 Exact results in the kondo problem: II. Scaling theory, qualitatively correct solution, and some new results on one-dimensional classical statistical models *Phys. Rev.* B **1** 4464–73
[45] Andrei N, Furuya K and Lowenstein J H 1983 Solution of the Kondo problem *Rev. Mod. Phys.* **55** 331–402
[46] Hewson A C 2000 *The Kondo Problem to Heavy Fermions* (Cambridge: Cambridge University Press)
[47] Costa A T Jr, Bose S and Omar Y 2006 Entanglement of two impurities through electron scattering *Phys. Rev. Lett.* **96** 230501
[48] Samuelsson P and Verdozzi C 2007 Two-particle spin entanglement in magnetic Anderson nanoclusters *Phys. Rev.* B **75** 132405
[49] Hu M-L 2008 Impurity entanglement in the open-ended Heisenberg chains *Mod. Phys. Lett.* **29** 2849–55
[50] Andrei N 1980 Diagonalization of the Kondo Hamiltonian *Phys. Rev. Lett.* **45** 379
[51] Wiegmann P B 1980 Exact solution of s–d exchange model at t = 0 *JETP Lett.* **31** 364
[52] Friedan D and Konechny A 2004 Boundary entropy of one-dimensional quantum systems at low temperature *Phys. Rev. Lett.* **93** 030402
[53] Laflorencie N, Sørensen E S and Affleck I 2008 The Kondo effect in spin chains *J. Stat. Mechanics: Theory Exp.* **02** P02007 (31 pp)
[54] Refael G and Moore J E 2004 Entanglement entropy of random quantum critical points in one dimension *Phys. Rev. Lett.* **93** 260602
[55] Alet F, Capponi S, Laflorencie N and Mambrini M 2007 Valence bond entanglement entropy *Phys. Rev. Lett.* **99** 117204
[56] Chhajlany R W, Tomczak P and Wojcik A 2007 Topological estimator of block entanglement for Heisenberg antiferromagnets *Phys. Rev. Lett.* **99** 167204
[57] Alet F and Laflorencie N 2009 Unpublished
[58] Fendley P, Fisher M P A and Nayak C 2007 Topological entanglement entropy from the holographic partition function *J. Stat. Phys.* **126** 1111

[59] Wen X-G 1990 Chiral Luttinger liquid and the edge excitations in the fractional quantum hall states *Phys. Rev.* B **41** 12838
[60] Wen X-G 1990 Electrodynamical properties of gapless edge excitations in the fractional quantum Hall states *Phys. Rev. Lett.* **64** 2206
[61] Wen X-G 1991 Gapless boundary excitations in the quantum Hall states and in the chiral spin states *Phys. Rev.* B **43** 11025
[62] Wen X-G 1991 Edge transport properties of the fractional quantum Hall states and weak-impurity scattering of a one-dimensional charge-density wave *Phys. Rev.* B **44** 5708
[63] Kane C L and Fisher M P A 1992 Transport in a one-channel Luttinger liquid *Phys. Rev. Lett.* **68** 1220
[64] Kane C L and Fisher M P A 1992 Resonant tunneling in an interacting one-dimensional electron gas *Phys. Rev.* B **46** 7268
[65] Furusaki A and Nagaosa N 1993 Resonant tunneling in a Luttinger liquid *Phys. Rev.* B **47** 3827
[66] Moon K, Yi H, Kane C L, Girvin S M and Fisher M P A 1993 Resonant tunneling between quantum Hall edge states *Phys. Rev. Lett.* **71** 4381
[67] Eisler V and Peschel I 2007 Evolution of entanglement after a local quench *J. Stat. Mech.* P06005
[68] Apollaro T J G and Plastina F 2006 Entanglement localization by a single defect in a spin chain *Phys. Rev.* A **74** 062316
[69] Apollaro T J, Cuccoli A, Fubini A, Plastina F and Verrucchi P 2008 Staggered magnetization and entanglement enhancement by magnetic impurities in a $s = (1/2)$ spin chain *Phys. Rev.* A **77** 062314
[70] Igloi F, Szatmári Z and Lin Y-C 2009 Entanglement entropy with localized and extended interface defects *Phys. Rev.* B **80** 024405
[71] Sakai K and Satoh Y 2008 Entanglement through conformal interfaces *J. High Energy Phys.* JHEP12(2008)001
[72] Franą V and Capelle K 2008 Entanglement in spatially inhomogeneous many-fermion systems *Phys. Rev. Lett.* **100** 070403
[73] Wang X 2004 Boundary and impurity effects on the entanglement of Heisenberg chains *Phys. Rev.* E **69** 066118
[74] Chung M-C and Peschel I 2001 Density-matrix spectra of solvable fermionic systems *Phys. Rev.* B **64** 064412
[75] Peschel I 2003 Calculation of reduced density matrices from correlation functions *J. Phys. A: Math. Gen.* **36** L205
[76] Peschel I and Eisler V 2009 Reduced density matrix and entanglement entropy for free lattice models *J. Phys. A: Math. Theor.* **42** 504003
[77] Jin B-Q and Korepin V E 2004 Quantum spin chain, Toeplitz determinants and Fisher–Hartwig conjecture *J. Stat. Phys.* **116** 79
[78] Legeza Ö, Sólyom J, Tincani L and Noack R M 2007 Entropic analysis of quantum phase transitions from uniform to spatially inhomogeneous phases *Phys. Rev. Lett.* **99** 087203
[79] Szirmai E, Legeza Ö and Sólyom J 2008 Spatially nonuniform phases in the one-dimensional su(n) Hubbard model for commensurate fillings *Phys. Rev.* B **77** 045106
[80] Roux G, Capponi S, Lecheminant P and Azaria P 2009 Spin 3/2 fermions with attractive interactions in a one-dimensional optical lattice: phase diagrams, entanglement entropy, and the effect of the trap *Eur. Phys. J.* B **68** 293
[81] Läuchli A and Kollath C 2008 Spreading of correlations and entanglement after a quench in the one-dimensional Bose–Hubbard model *J. Stat. Mech.* P05018
[82] Jacobsen J L and Saleur H 2008 Exact valence bond entanglement entropy and probability distribution in the xxx spin chain and the Potts model *Phys. Rev. Lett.* **100** 087205
[83] Kallin A B, González I, Hastings M B and Melko R G 2009 Valence bond and von Neumann entanglement entropy in Heisenberg ladders *Phys. Rev. Lett.* **103** 117203
[84] Sandvik A W 2005 Ground state projection of quantum spin systems in the valence bond basis *Phys. Rev. Lett.* **95** 207203
[85] Laflorencie N 2005 Scaling of entanglement entropy in the random singlet phase *Phys. Rev.* B **72** 140408(R)
[86] Hoyos J A, Vieira A P, Laflorencie N and Miranda E 2007 Correlation amplitude and entanglement entropy in random spin chains *Phys. Rev.* B **76** 174425
[87] Tsai S W and Marston J B 2000 Density-matrix renormalization-group analysis of quantum critical points: I. Quantum spin chains *Phys. Rev.* B **62** 5546
[88] Barzykin V and Affleck I 1999 Finite-size scaling for the $s = 1/2$ Heisenberg antiferromagnetic chain *J. Phys. A: Math. Gen.* **32** 867
[89] Castro-Alvaredo O A and Doyon B 2009 Bi-partite entanglement entropy in massive 1+1-dimensional quantum field theories *J. Phys. A: Math Theor.* **42** 504006
[90] Fan H, Korepin V and Roychowdhury V 2004 Entanglement in a valence-bond solid state *Phys. Rev. Lett.* **93** 227203

[91] Fan H, Korepin V, Roychowdhury V, Hadley C and Bose S 2007 Boundary effects and two-site entanglement of the spin-1 valence-bond solid *Phys. Rev.* B **76** 014428 (arXiv:quant-ph/0605133)
[92] Affleck I, Kennedy T, Lieb E H and Tasaki H 1987 Rigorous results on valence-bond ground states in antiferromagnets *Phys. Rev. Lett.* **59** 799–802
[93] Affleck I, Kennedy T, Lieb E H and Tasaki H 1988 Valence bond ground states in isotropic quantum antiferromagnets *Commun. Math. Phys.* **115** 477–528
[94] Majumdar C K 1970 Antiferromagnetic model with known ground state *J. Phys. C: Solid State Phys.* **3** 911
[95] Majumdar C K and Ghosh D K 1969 On next-nearest-neighbor interaction in linear chain: I *J. Math. Phys.* **10** 1388
[96] Majumdar C K and Ghosh D K 1969 On next-nearest-neighbor interaction in linear chain: II *J. Math. Phys.* **10** 1399
[97] Shastry B S and Sutherland B 1981 Excitation spectrum of a dimerized next-neighbor antiferromagnetic chain *Phys. Rev. Lett.* **47** 964
[98] Caspers W J and Magnus W 1982 Some exact excited states in a linear antiferromagnetic spin system *Phys. Lett.* A **88** 103
[99] Caspers W J, Emmett K M and Magnus W 1984 The Majumdar-Ghosh chain. Twofold ground state and elementary excitations *J. Phys. A: Math. Gen.* **17** 2687
[100] Sørensen E S, Affleck I, Augier D and Poilblanc D 1998 Soliton approach to spin-Peierls antiferromagnets: large-scale numerical results *Phys. Rev.* B **58** 14701
[101] Uhrig G S, Schönfeld F, Laukamp M and Dagotto E 1999 Unified quantum mechanical picture for confined spinons in dimerized and frustrated $s = 1/2$ chains *Eur. Phys. J.* B **7** 67–77
[102] Doretto R L and Vojta M 2009 Quantum magnets with weakly confined spinons: multiple length scales and quantum impurities *Phys. Rev.* B **80** 024411
[103] Sørensen E S 1998 Parity, precision and spin-inversion within the DMRG *J. Phys. Cond. Matt.* **10** 10655